CASL-U-2016-1164-000
ORNL/SR-2016/360

# Assessment of the MPACT Resonance Data Generation Procedure

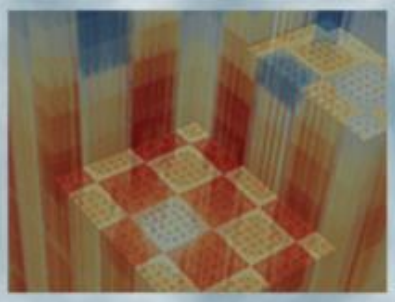
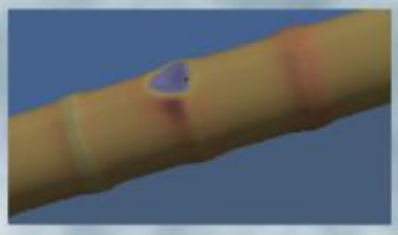
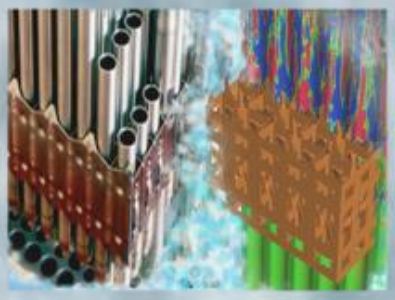

Revision 0

Kang Seog Kim
Mark L. Williams

**December 26, 2016**

A DOE Energy Innovation Hub

U.S. DEPARTMENT OF ENERGY | Nuclear Energy

## REVISION LOG

| Revision | Date | Affected Pages | Revision Description |
|---|---|---|---|
| 0 | 12/26/2016 | All | Initial version |
| | | | |
| | | | |
| | | | |

Export Controlled None

IP/Proprietary/NDA Controlled None

Sensitive Controlled None

Unlimited All Pages

**Requested Distribution:**

To: N/A

Copy: N/A

**Reviewed by:**

Date:

Reviewer: Kevin T. Clarno, Cihangir Celik

## EXECUTIVE SUMMARY

Currently, heterogeneous models are being used to generate resonance self-shielded cross-section tables as a function of background cross sections for important nuclides such as $^{235}U$ and $^{238}U$ by performing the CENTRM (Continuous Energy Transport Model) slowing down calculation with the MOC (Method of Characteristics) spatial discretization and ESSM (Embedded Self-Shielding Method) calculations to obtain background cross sections. And then the resonance self-shielded cross section tables are converted into subgroup data which are to be used in estimating problem-dependent self-shielded cross sections in MPACT (Michigan Parallel Characteristics Transport Code). Although this procedure has been developed and thus resonance data have been generated and validated by benchmark calculations, assessment has never been performed to review if the resonance data are properly generated by the procedure and utilized in MPACT. This study focuses on assessing the procedure and a proper use in MPACT.

# TABLE OF CONTENTS

## FIGURES

# TABLES

## ACRONYMS

| | |
|---|---|
| 0D | Zero-Dimensional (Homogeneous) |
| 1D | One-Dimensional |
| 2D | Two-Dimensional |
| BWR | Boiling Water Reactor |
| CASL | Consortium for Advanced Simulation of Light Water Reactors |
| CE | Continuous Energy (as in cross sections) |
| CENTRM | Continuous Energy Transport Model |
| ESSM | Embedded Self-Shielding Method |
| IR | Intermediate Resonance |
| MG | Multi-group (as in cross sections) |
| MOC | Method of Characteristics |
| MPACT | Michigan Parallel Characteristics Transport Code |
| NR | Marrow Resonance |
| ORNL | Oak Ridge National Laboratory |
| PW | Pointwise |
| PWR | Pressurized Water Reactor |
| RI | Resonance Integral |
| URR | Unresolved resonance |
| WR | Wide Resonance |
| XS | Cross Section |

# 1 INTRODUCTION

Currently, heterogeneous models are being used to generate resonance self-shielded cross-section tables as a function of background cross sections by performing the CENTRM (Continuous Energy Transport Model) [Wil06] slowing down calculation with the MOC (Method of Characteristics) spatial discretization and ESSM (Embedded Self-Shielding Method) [Wil12] calculations to obtain background cross sections by using the SCALE IRFFACTOR [Rea16]. The resonance self-shielded cross section tables are then converted into subgroup data by using SUBGR [Kim16a] which are to be used in estimating problem dependent self-shielded cross sections in MPACT (Michigan Parallel Characteristics Transport Code). All of programs and procedures include unit and regression tests for verification under the SCALE and AMPX [Wia16] SQA procedure. Although this procedure has been developed and thus resonance data have been generated, assessment has never been performed to review if the resonance data are properly generated by the procedure and correctly utilized in MPACT. This study focuses on assessing the procedure and a proper use in MPACT, including the following.

- Are the CENTRM slowing down calculations with MOC and Sn (Discrete Ordinate Method) working correctly?
- Are the corresponding background cross sections correctly obtained by performing the ESSM fixed source calculations?
- Are the self-shielded cross sections estimated by using subgroup method in MPACT acceptable?

# 2 CENTRM SLOWING DOWN CALCULATION

## 2.1 BENCHMARK PROBLEMS

Tables 2.1 and 2.2 provide Pressurized Water Reactor (PWR) and Boiling Water Reactor (BWR) pin cell configurations including geometry and composition, respectively, which are used in benchmark calculations. The CENTRM slowing down pointwise (PW) calculations are performed by 1D cylindrical Sn or 2D square MOC as shown in Figure 2.1 to obtain the effective multi-group (MG) cross sections to be used in the following eigenvalue transport calculations by using XSDRN, NEWT and KENO-MG.

**Table 2.1 PWR pin cell configuration**

| Region | Material | Radius (cm) | Temperature (K) | Atomic density | |
|---|---|---|---|---|---|
| Fuel | $UO_2$ | 0.40250 | 293.6 / 600.0 | $^{235}U$ | 9.39467E-4 |
| | | | | $^{238}U$ | 2.22624E-2 |
| | | | | $^{16}O$ | 4.64223E-2 |
| Clad | Al | 0.47590 | 293.6 / 600.0 | $^{27}Al$ | 6.02611E-2 |
| Moderator | $H_2O$ | 1.26200 (pitch) | 293.6 | $^{1}H$ | 6.72142E-2 |
| | | | | $^{16}O$ | 3.36071E-2 |
| | | | 600.0 | $^{1}H$ | 4.41833E-2 |
| | | | | $^{16}O$ | 2.20950E-2 |

**Table 2.2 BWR pin cell configuration**

| Region | Material | Radius (cm) | Temperature (K) | Atomic density | |
|---|---|---|---|---|---|
| Fuel | $UO_2$ | 0.60579 | 293.6 / 600.0 | $^{235}U$ | 9.39467E-4 |
| | | | | $^{238}U$ | 2.22624E-2 |
| | | | | $^{16}O$ | 4.64223E-2 |
| Clad | Al | 0.62103 | 293.6 / 600.0 | $^{27}Al$ | 6.02611E-2 |
| Moderator | $H_2O$ | 1.87452 (pitch) | 293.6 | $^{1}H$ | 6.72142E-2 |
| | | | | $^{16}O$ | 3.36071E-2 |
| | | | 600.0 | $^{1}H$ | 4.41833E-2 |
| | | | | $^{16}O$ | 2.20950E-2 |

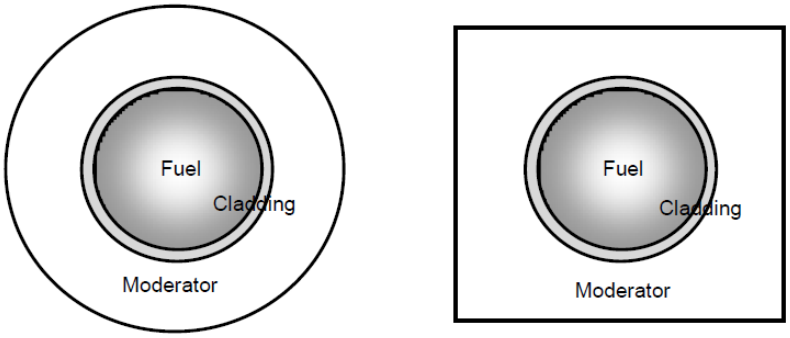


**Figure 2.1 Wigner-Seitz cylindrical and square pin cell models.**

## 2.2 CALCULATION CASES

The benchmark problems considered include two PWR and two BWR cases at two different temperatures (293.6 and 600 K), for which KENO-CE, CENTRM-MOC+KENO-MG and CENTRM-Sn+KENO-MG calculations have been performed with the ENDF/B-7.0 and 7.1 continuous energy cross section and 51 and 252-group libraries.

- Case A. PWR 293.6 K
- Case B. PWR 600.0 K
- Case C. BWR 293.6 K
- Case D. BWR 600.0 K

Appendices A, B and C provide the SCALE sample inputs for KENO-CE, CENTRM-MOC+KENO-MG and CENTRM-Sn+KENO-MG calculations.

## 2.3 RESULTS AND ANALYSIS

Tables 2.3 and 2.4 provide comparisons of the multiplication factors between KENO-CE and CENTRM/KENO-MG when using the MPACT 51 and 252-g libraries [Kim16b]. Both CENTRM-MOC and Sn underestimate the multiplication factors, and CENTRM-MOC predictions are better than CENTRM-Sn by 60 pcm for 252-g and more than 100 pcm for 51-g. The trend of results is consistent with that obtained with old versions of SCALE in 2014. However, the reactivity difference between CENTRM-MOC and Sn is different from the earlier results, which were about 100 to 160 pcm for 252-g.

**Table 2.3 Comparison of the multiplication factors (51-group)**

| ENDF/B | Case | Keff | | | Reactivity diff. (pcm) | |
|---|---|---|---|---|---|---|
| | | KENO-CE [a] | CENTRM-MOC [b] | CENTRM-Sn [c] | [b]-[a] | [c]-[a] |
| 7.0 | A. PWR 300 K | 1.45798 | 1.45469 | 1.45221 | -155 | -273 |
| | B. PWR 600 K | 1.37383 | 1.36996 | 1.36658 | -206 | -386 |
| | C. BWR 300 K | 1.49106 | 1.48972 | 1.48813 | -60 | -132 |
| | D. BWR 600 K | 1.43293 | 1.42946 | 1.42743 | -170 | -269 |
| 7.1 | A. PWR 300 K | 1.45768 | 1.45476 | 1.45217 | -138 | -260 |
| | B. PWR 600 K | 1.37361 | 1.37010 | 1.36657 | -187 | -375 |
| | C. BWR 300 K | 1.49101 | 1.48964 | 1.48812 | -62 | -130 |
| | D. BWR 600 K | 1.43278 | 1.42960 | 1.42725 | -155 | -270 |

**Table 2.4 Comparison of the multiplication factors (252-group)**

| ENDF/B | Case | Keff | | | Reactivity diff. (pcm) | |
|---|---|---|---|---|---|---|
| | | KENO-CE [a] | CENTRM-MOC [b] | CENTRM-Sn [c] | [b]-[a] | [c]-[a] |
| 7.0 | A. PWR 300 K | 1.45798 | 1.45567 | 1.45434 | -109 | -172 |
| | B. PWR 600 K | 1.37383 | 1.37180 | 1.37051 | -108 | -176 |
| | C. BWR 300 K | 1.49106 | 1.48946 | 1.48891 | -72 | -97 |
| | D. BWR 600 K | 1.43293 | 1.43154 | 1.43033 | -68 | -127 |
| 7.1 | A. PWR 300 K | 1.45768 | 1.45541 | 1.45431 | -107 | -159 |
| | B. PWR 600 K | 1.37361 | 1.37181 | 1.37037 | -95 | -172 |
| | C. BWR 300 K | 1.49101 | 1.48939 | 1.48864 | -73 | -107 |
| | D. BWR 600 K | 1.43278 | 1.43136 | 1.43023 | -69 | -124 |

Reactivity (reaction rate) analysis between KENO-CE and CENTRM/KENO-MG has been carried out by using the following procedure.

a. KENO-CE calculation
   Edit 51-g/252-g scalar fluxes, microscopic capture and fission cross sections, the number of neutrons (ν) released from a fission, and the multiplication factors.

b. XSPROC (BONAMI/CENTRM/PMC) calculation (MOC and Sn options)
   Edit 51-g/252-g microscopic capture and fission cross sections from PMC output.

c. KENO-MG calculation
   Edit 51-g/252-g scalar fluxes and the multiplication factors from the KENO-MG output.

d. Comparison and conversion
   Compare multiplication factors and convert the differences of cross sections and scalar fluxes into reactivity differences: $U^{235}$ and $U^{238}$ absorption and ν*fission, and overall. (Refer to the following paragraph) Same ν's have been used.

Absorption and ν*fission reaction rate differences between KENO-CE and CENTRM/KENO-MG for $U^{235}$ are converted into the reactivity differences in *pcm* for each group by using the following equations.

$$\Delta\rho_{a,g'}^{235} = \left[\frac{1}{k_\infty} - \frac{\sum_{g,k} N_k \sigma_{a,g,k}\phi_g - N^{235}\left(\sigma_{a,g'}^{235}\phi_{g'} - \hat{\sigma}_{a,g'}^{235}\hat{\phi}_{g'}\right)}{\sum_{g,k} N_k \nu\sigma_{f,g,k}\phi_g}\right]\cdot 10^5, \qquad (2.1)$$

and

$$\Delta\rho_{\nu f,g'}^{235} = \left[\frac{1}{k_\infty} - \frac{\sum_{g,k} N_k \sigma_{a,g,k}\phi_g}{\sum_{g,k} N_k \nu\sigma_{f,g,k}\phi_g - N^{235}(\nu\sigma_{f,g'}^{235}\phi_{g'} - \nu\hat{\sigma}_{f,g'}^{235}\hat{\phi}_{g'}}\right]\cdot 10^5, \qquad (2.2)$$

where

$$k_\infty = \frac{\sum_{g,k} N_k \nu\sigma_{f,g,k}\phi_g}{\sum_{g,k} N_k \sigma_{a,g,k}\,\phi_g},$$

and cap(^) indicates data from the CENTRM/KENO-MG calculations, k denotes fissionable nuclide and *g* energy group. To see the effect of cross section differences, the CENTRM/KENO-MG scalar flux needs to be replaced with the KENO-CE scalar flux.

In addition three-group reactivity analysis has been performed by using the following group structure.

- Fast energy group: 9.5 keV – 20 MeV
- Resolved resonance energy group: 1.01 eV – 9.5 keV
- Thermal energy group: 0.0 eV – 1.01 eV

Tables 2.5~2.12 provide the results of the 3-group reactivity analysis results for the PWR and BWR fuel pin cell problems by using the ENDF/B-7.0 and 7.1 MPACT 51 and 252-g libraries.

Two different reactivity analyses have been carried out to see the reactivity changes due to either cross-section difference or cross-section plus scalar flux difference. The analysis summary is as follows:

a. Large reactivity differences at $^{235}$U thermal and $^{238}$U resolved resonance groups.

b. Error cancellation between absorption and $\nu$*fission at $^{235}$U thermal group.

c. Roughly similar reactivity differences due to only the cross-section differences at the $^{238}$U resolved resonance group, but the direction is opposite.

d. When considering both effect of cross section and scalar flux, CENTRM-MOC provides better results than CENTRM-Sn by 60 pcm for all cases when using 252-group structure. This indicates that the CENTRM-MOC can produce better scattering matrices to result in better scalar fluxes.

e. When using the 51-group structure, both cross section and scalar flux differences result in reactivity differences which indicates that the 51-group structure needs to be optimized.

f. While the 252-g results do not introduce any reactivity bias for temperature, the 51-g structure introduce significant reactivity bias for fuel temperature as indicated in the CASL VERA-CS MPACT calculations based on Bondarenko approach. This temperature bias comes from the U-235 thermal and U-238 resonances.

g. CENTRM-MOC provides better results than CENTRM-Sn by 60 pcm for all cases when using 252-group structure. This indicates that the CENTRM-MOC can produce better scattering matrices to result in better scalar fluxes.

h. The quality of $^{235}$U 1D cross sections is very good. However, the quality of thermal spectra is not good and then results in large reactivity differences. Fortunately, there are error cancellations between absorption and $\nu$*fission reactions.

**Table 2.5 Three-group reactivity analysis for the PWR fuel pins (ENDF/B-7.0, 51-g)**

| Case | | Group | XS effect | | | | | XS/Flux effect | | | | |
|---|---|---|---|---|---|---|---|---|---|---|---|---|
| | | | $^{235}U$ | | $^{238}U$ | | Sum | $^{235}U$ | | $^{238}U$ | | Sum |
| | | | $R_a$ | $R_{nf}$ | $R_a$ | $R_{nf}$ | | $R_a$ | $R_{nf}$ | $R_a$ | $R_{nf}$ | |
| PWR 300 K | MOC | Fast | 0 | 0 | 1 | -2 | 0 | 0 | 0 | 3 | -5 | -2 |
| | | RR | 5 | -4 | -27 | 0 | -27 | -3 | 0 | -110 | 0 | -113 |
| | | Thermal | 186 | -244 | 6 | 0 | -52 | 225 | -294 | 8 | 0 | -60 |
| | | Sum | 191 | -249 | -20 | -2 | -79 | 222 | -294 | -98 | -5 | -175 |
| | Sn | Fast | 0 | 0 | 1 | -2 | -1 | 0 | 0 | 1 | -4 | -3 |
| | | RR | -10 | 9 | -171 | 0 | -173 | -9 | 5 | -225 | 0 | -229 |
| | | Thermal | 195 | -256 | 7 | 0 | -54 | 284 | -373 | 14 | 0 | -75 |
| | | Sum | 185 | -247 | -164 | -2 | -228 | 275 | -368 | -210 | -4 | -306 |
| PWR 600 K | MOC | Fast | 0 | 0 | 1 | 2 | 2 | -2 | 2 | -5 | 7 | 3 |
| | | RR | 5 | -6 | -47 | 0 | -48 | 3 | -7 | -123 | 0 | -127 |
| | | Thermal | 30 | -43 | -1 | 0 | -15 | 244 | -349 | 22 | 0 | -83 |
| | | Sum | 35 | -49 | -48 | 2 | -60 | 245 | -353 | -106 | 7 | -207 |
| | Sn | Fast | 0 | 0 | 0 | 2 | 2 | -2 | 4 | -9 | 10 | 2 |
| | | RR | -14 | 12 | -255 | 0 | -257 | 3 | -8 | -282 | 0 | -287 |
| | | Thermal | 29 | -42 | -1 | 0 | -14 | 313 | -449 | 30 | 0 | -107 |
| | | Sum | 16 | -31 | -256 | 2 | -269 | 314 | -453 | -261 | 10 | -391 |

**Table 2.6 Three-group reactivity analysis for the BWR fuel pins (ENDF/B-7.0, 51-g)**

| Case | | Group | XS effect | | | | | XS/Flux effect | | | | |
|---|---|---|---|---|---|---|---|---|---|---|---|---|
| | | | $^{235}U$ | | $^{238}U$ | | Sum | $^{235}U$ | | $^{238}U$ | | Sum |
| | | | $R_a$ | $R_{nf}$ | $R_a$ | $R_{nf}$ | | $R_a$ | $R_{nf}$ | $R_a$ | $R_{nf}$ | |
| BWR 300 K | MOC | Fast | 0 | 0 | 1 | -3 | -2 | 1 | -1 | 8 | -13 | -5 |
| | | RR | 9 | -8 | -6 | 0 | -5 | -5 | 3 | -78 | 0 | -80 |
| | | Thermal | 161 | -203 | 4 | 0 | -39 | 175 | -220 | 3 | 0 | -42 |
| | | Sum | 170 | -211 | -1 | -3 | -45 | 171 | -218 | -67 | -13 | -128 |
| | Sn | Fast | 0 | 0 | 1 | -3 | -2 | 0 | -1 | 6 | -10 | -4 |
| | | RR | -2 | 1 | -85 | 0 | -86 | -11 | 8 | -137 | 0 | -139 |
| | | Thermal | 189 | -239 | 6 | 0 | -44 | 215 | -271 | 7 | 0 | -49 |
| | | Sum | 187 | -237 | -78 | -3 | -132 | 205 | -264 | -124 | -10 | -193 |
| BWR 600 K | MOC | Fast | 0 | 0 | 0 | -1 | -1 | -1 | 1 | 3 | -8 | -4 |
| | | RR | 9 | -9 | -31 | 0 | -31 | -9 | 8 | -111 | 0 | -112 |
| | | Thermal | 20 | -27 | -2 | 0 | -9 | 229 | -314 | 21 | 0 | -64 |
| | | Sum | 28 | -35 | -32 | -1 | -41 | 220 | -305 | -87 | -7 | -180 |
| | Sn | Fast | 0 | 0 | 0 | -1 | -1 | -1 | 2 | -1 | -3 | -3 |
| | | RR | -8 | 6 | -156 | 0 | -158 | -12 | 9 | -205 | 0 | -207 |
| | | Thermal | 23 | -31 | -2 | 0 | -10 | 273 | -375 | 26 | 0 | -76 |
| | | Sum | 15 | -25 | -158 | -1 | -169 | 260 | -364 | -180 | -3 | -287 |

**Table 2.7 Three-group reactivity analysis for the PWR fuel pins (ENDF/B-7.1, 51-g)**

| Case | | Group | XS effect | | | | | XS/Flux effect | | | | |
|---|---|---|---|---|---|---|---|---|---|---|---|---|
| | | | $^{235}U$ | | $^{238}U$ | | Sum | $^{235}U$ | | $^{238}U$ | | Sum |
| | | | $R_a$ | $R_{nf}$ | $R_a$ | $R_{nf}$ | | $R_a$ | $R_{nf}$ | $R_a$ | $R_{nf}$ | |
| PWR 300 K | MOC | Fast | -3 | 4 | 2 | -2 | 0 | -3 | 4 | 4 | -4 | -1 |
| | | RR | 3 | -1 | -26 | 0 | -24 | -4 | 3 | -106 | 0 | -107 |
| | | Thermal | 180 | -235 | 5 | 0 | -50 | 223 | -292 | 8 | 0 | -60 |
| | | Sum | 180 | -232 | -19 | -2 | -73 | 216 | -285 | -94 | -4 | -167 |
| | Sn | Fast | -3 | 4 | 1 | -2 | 0 | -4 | 4 | 1 | -2 | -1 |
| | | RR | -12 | 12 | -169 | 0 | -169 | -11 | 9 | -216 | 0 | -218 |
| | | Thermal | 188 | -246 | 6 | 0 | -52 | 288 | -378 | 15 | 0 | -75 |
| | | Sum | 172 | -229 | -162 | -2 | -221 | 273 | -365 | -201 | -2 | -295 |
| PWR 600 K | MOC | Fast | -5 | 6 | 2 | 1 | 4 | -7 | 9 | -4 | 8 | 6 |
| | | RR | -2 | 5 | -37 | 0 | -34 | -3 | 4 | -112 | 0 | -112 |
| | | Thermal | 27 | -39 | -2 | 0 | -13 | 241 | -345 | 22 | 0 | -82 |
| | | Sum | 20 | -27 | -37 | 1 | -43 | 231 | -332 | -94 | 8 | -188 |
| | Sn | Fast | -5 | 6 | 1 | 1 | 4 | -8 | 10 | -8 | 10 | 4 |
| | | RR | -20 | 23 | -245 | 0 | -242 | -3 | 3 | -272 | 0 | -272 |
| | | Thermal | 26 | -38 | -2 | 0 | -13 | 319 | -459 | 30 | 0 | -109 |
| | | Sum | 1 | -9 | -245 | 1 | -252 | 308 | -445 | -249 | 10 | -377 |

**Table 2.8 Three-group reactivity analysis for the BWR fuel pins (ENDF/B-7.1, 51-g)**

| Case | | Group | XS effect | | | | | XS/Flux effect | | | | |
|---|---|---|---|---|---|---|---|---|---|---|---|---|
| | | | $^{235}U$ | | $^{238}U$ | | Sum | $^{235}U$ | | $^{238}U$ | | Sum |
| | | | $R_a$ | $R_{nf}$ | $R_a$ | $R_{nf}$ | | $R_a$ | $R_{nf}$ | $R_a$ | $R_{nf}$ | |
| BWR 300 K | MOC | Fast | -3 | 3 | 2 | -3 | -1 | -2 | 2 | 8 | -11 | -3 |
| | | RR | 5 | -2 | -11 | 0 | -8 | -11 | 11 | -82 | 0 | -82 |
| | | Thermal | 153 | -193 | 3 | 0 | -37 | 188 | -237 | 4 | 0 | -45 |
| | | Sum | 155 | -192 | -6 | -3 | -46 | 175 | -224 | -70 | -11 | -130 |
| | Sn | Fast | -3 | 3 | 1 | -3 | -1 | -2 | 2 | 6 | -9 | -3 |
| | | RR | -7 | 8 | -90 | 0 | -89 | -16 | 16 | -144 | 0 | -144 |
| | | Thermal | 181 | -228 | 5 | 0 | -42 | 235 | -297 | 9 | 0 | -53 |
| | | Sum | 171 | -217 | -83 | -3 | -132 | 216 | -279 | -129 | -9 | -201 |
| BWR 600 K | MOC | Fast | -5 | 5 | 1 | -1 | 1 | -5 | 6 | 3 | -5 | -1 |
| | | RR | 3 | 0 | -23 | 0 | -21 | -12 | 12 | -102 | 0 | -101 |
| | | Thermal | 16 | -22 | -2 | 0 | -8 | 212 | -290 | 19 | 0 | -59 |
| | | Sum | 14 | -17 | -24 | -1 | -28 | 195 | -271 | -81 | -5 | -161 |
| | Sn | Fast | -5 | 5 | 1 | -1 | 0 | -6 | 7 | 0 | -2 | -1 |
| | | RR | -14 | 15 | -148 | 0 | -148 | -21 | 21 | -199 | 0 | -199 |
| | | Thermal | 19 | -26 | -2 | 0 | -9 | 282 | -387 | 26 | 0 | -79 |
| | | Sum | 1 | -6 | -150 | -1 | -156 | 255 | -359 | -173 | -2 | -279 |

**Table 2.9 Three-group reactivity analysis for the PWR fuel pins (ENDF/B-7.0, 252-g)**

| Case | | Group | XS effect | | | | | XS/Flux effect | | | | |
|---|---|---|---|---|---|---|---|---|---|---|---|---|
| | | | $^{235}U$ | | $^{238}U$ | | Sum | $^{235}U$ | | $^{238}U$ | | Sum |
| | | | $R_a$ | $R_{nf}$ | $R_a$ | $R_{nf}$ | | $R_a$ | $R_{nf}$ | $R_a$ | $R_{nf}$ | |
| PWR 300 K | MOC | Fast | 0 | 0 | 0 | 0 | 1 | 0 | 0 | 1 | -2 | -1 |
| | | RR | -1 | 1 | 30 | 0 | 31 | 7 | -6 | -96 | 0 | -95 |
| | | Thermal | -10 | 12 | -1 | 0 | 2 | 79 | -105 | 7 | 0 | -19 |
| | | Sum | -11 | 14 | 30 | 0 | 33 | 86 | -111 | -88 | -2 | -115 |
| | Sn | Fast | 0 | 0 | 0 | 0 | 0 | 0 | 0 | 0 | -1 | -1 |
| | | RR | -11 | 10 | -54 | 0 | -55 | 1 | -2 | -148 | 0 | -148 |
| | | Thermal | -8 | 10 | -1 | 0 | 2 | 103 | -136 | 9 | 0 | -25 |
| | | Sum | -19 | 20 | -55 | 0 | -53 | 104 | -138 | -139 | -1 | -174 |
| PWR 600 K | MOC | Fast | 0 | 0 | 0 | 1 | 1 | 0 | 0 | -1 | 0 | 0 |
| | | RR | 0 | 1 | 39 | 0 | 40 | 15 | -14 | -91 | 0 | -91 |
| | | Thermal | 0 | 0 | 0 | 0 | 0 | 47 | -66 | 6 | 0 | -13 |
| | | Sum | 0 | 1 | 39 | 1 | 41 | 62 | -80 | -86 | 0 | -104 |
| | Sn | Fast | 0 | 0 | 0 | 1 | 1 | -1 | 1 | -4 | 4 | 0 |
| | | RR | -11 | 12 | -73 | 0 | -73 | 12 | -12 | -147 | 0 | -147 |
| | | Thermal | -1 | 1 | 0 | 0 | 0 | 71 | -100 | 8 | 0 | -21 |
| | | Sum | -12 | 12 | -74 | 1 | -72 | 82 | -111 | -143 | 4 | -168 |

**Table 2.10 Three-group reactivity analysis for the BWR fuel pins (ENDF/B-7.0, 252-g)**

| Case | | Group | XS effect | | | | | XS/Flux effect | | | | |
|---|---|---|---|---|---|---|---|---|---|---|---|---|
| | | | $^{235}U$ | | $^{238}U$ | | Sum | $^{235}U$ | | $^{238}U$ | | Sum |
| | | | $R_a$ | $R_{nf}$ | $R_a$ | $R_{nf}$ | | $R_a$ | $R_{nf}$ | $R_a$ | $R_{nf}$ | |
| BWR 300 K | MOC | Fast | 0 | 0 | 0 | 0 | 0 | 1 | -1 | 4 | -6 | -2 |
| | | RR | 2 | -2 | 40 | 0 | 40 | 6 | -5 | -66 | 0 | -65 |
| | | Thermal | -21 | 26 | -2 | 0 | 4 | 55 | -70 | 4 | 0 | -11 |
| | | Sum | -19 | 25 | 38 | 0 | 44 | 62 | -76 | -58 | -6 | -78 |
| | Sn | Fast | 0 | 0 | 0 | 0 | 0 | 0 | -1 | 3 | -4 | -1 |
| | | RR | -5 | 4 | -15 | 0 | -16 | 2 | -3 | -90 | 0 | -91 |
| | | Thermal | -8 | 10 | -1 | 0 | 1 | 66 | -84 | 5 | 0 | -13 |
| | | Sum | -13 | 14 | -16 | 0 | -15 | 69 | -87 | -83 | -4 | -105 |
| BWR 600 K | MOC | Fast | 0 | 0 | 0 | 1 | 1 | 0 | 0 | 3 | -4 | -2 |
| | | RR | 2 | -1 | 45 | 0 | 46 | 12 | -10 | -70 | 0 | -68 |
| | | Thermal | -2 | 3 | 0 | 0 | 1 | 43 | -57 | 5 | 0 | -9 |
| | | Sum | 0 | 2 | 45 | 1 | 48 | 55 | -68 | -61 | -4 | -78 |
| | Sn | Fast | 0 | 0 | 0 | 1 | 0 | 0 | 0 | 1 | -3 | -2 |
| | | RR | -7 | 8 | -35 | 0 | -35 | 11 | -11 | -113 | 0 | -113 |
| | | Thermal | 0 | 0 | 0 | 0 | 0 | 74 | -100 | 9 | 0 | -17 |
| | | Sum | -7 | 7 | -35 | 1 | -34 | 85 | -111 | -104 | -3 | -133 |

**Table 2.11 Three-group reactivity analysis for the PWR fuel pins (ENDF/B-7.1, 252-g)**

| Case | | Group | XS effect | | | | | XS/Flux effect | | | | |
|---|---|---|---|---|---|---|---|---|---|---|---|---|
| | | | $^{235}U$ | | $^{238}U$ | | Sum | $^{235}U$ | | $^{238}U$ | | Sum |
| | | | $R_a$ | $R_{nf}$ | $R_a$ | $R_{nf}$ | | $R_a$ | $R_{nf}$ | $R_a$ | $R_{nf}$ | |
| PWR 300 K | MOC | Fast | -3 | 4 | 1 | 0 | 2 | -3 | 4 | 2 | -2 | 1 |
| | | RR | -5 | 7 | 35 | 0 | 37 | 2 | 0 | -97 | 0 | -95 |
| | | Thermal | -9 | 12 | -1 | 0 | 2 | 82 | -109 | 7 | 0 | -20 |
| | | Sum | -18 | 23 | 35 | 0 | 41 | 82 | -106 | -88 | -2 | -114 |
| | Sn | Fast | -3 | 4 | 0 | 0 | 1 | -3 | 4 | 0 | -1 | 0 |
| | | RR | -15 | 16 | -49 | 0 | -49 | -2 | 3 | -143 | 0 | -142 |
| | | Thermal | -7 | 9 | -1 | 0 | 1 | 111 | -147 | 10 | 0 | -26 |
| | | Sum | -26 | 29 | -49 | 0 | -46 | 105 | -140 | -133 | -1 | -169 |
| PWR 600 K | MOC | Fast | -5 | 6 | 1 | 1 | 3 | -6 | 7 | 0 | 0 | 1 |
| | | RR | -11 | 15 | 40 | 0 | 44 | 8 | -3 | -75 | 0 | -71 |
| | | Thermal | 0 | 0 | 0 | 0 | 0 | 47 | -66 | 6 | 0 | -13 |
| | | Sum | -16 | 21 | 41 | 1 | 47 | 50 | -63 | -69 | 0 | -82 |
| | Sn | Fast | -5 | 6 | 1 | 1 | 3 | -6 | 7 | -2 | 2 | 2 |
| | | RR | -22 | 26 | -72 | 0 | -69 | 3 | 0 | -149 | 0 | -146 |
| | | Thermal | -1 | 1 | 0 | 0 | 0 | 77 | -109 | 9 | 0 | -23 |
| | | Sum | -28 | 33 | -72 | 1 | -66 | 74 | -101 | -142 | 2 | -167 |

**Table 2.12 Three-group reactivity analysis for the BWR fuel pins (ENDF/B-7.1, 252-g)**

| Case | | Group | XS effect | | | | | XS/Flux effect | | | | |
|---|---|---|---|---|---|---|---|---|---|---|---|---|
| | | | $^{235}U$ | | $^{238}U$ | | Sum | $^{235}U$ | | $^{238}U$ | | Sum |
| | | | $R_a$ | $R_{nf}$ | $R_a$ | $R_{nf}$ | | $R_a$ | $R_{nf}$ | $R_a$ | $R_{nf}$ | |
| BWR 300 K | MOC | Fast | -3 | 3 | 1 | 0 | 1 | -2 | 2 | 4 | -4 | 0 |
| | | RR | -3 | 5 | 40 | 0 | 41 | -1 | 3 | -71 | 0 | -68 |
| | | Thermal | -21 | 27 | -2 | 0 | 4 | 66 | -84 | 5 | 0 | -13 |
| | | Sum | -27 | 35 | 39 | 0 | 46 | 63 | -79 | -61 | -4 | -81 |
| | Sn | Fast | -3 | 3 | 1 | 0 | 1 | -2 | 2 | 3 | -4 | -1 |
| | | RR | -10 | 11 | -15 | 0 | -15 | -3 | 5 | -101 | 0 | -99 |
| | | Thermal | -8 | 10 | -1 | 0 | 1 | 92 | -117 | 7 | 0 | -18 |
| | | Sum | -21 | 24 | -15 | 0 | -12 | 86 | -110 | -90 | -4 | -117 |
| BWR 600 K | MOC | Fast | -4 | 5 | 1 | 1 | 2 | -4 | 5 | 3 | -3 | 0 |
| | | RR | -6 | 8 | 50 | 0 | 52 | 5 | -1 | -63 | 0 | -59 |
| | | Thermal | -2 | 3 | 0 | 0 | 1 | 49 | -66 | 6 | 0 | -11 |
| | | Sum | -12 | 16 | 51 | 1 | 55 | 50 | -63 | -54 | -3 | -70 |
| | Sn | Fast | -4 | 5 | 1 | 1 | 2 | -4 | 5 | 2 | -2 | 0 |
| | | RR | -15 | 17 | -30 | 0 | -29 | 3 | 0 | -111 | 0 | -108 |
| | | Thermal | 0 | 0 | 0 | 0 | 0 | 57 | -76 | 7 | 0 | -13 |
| | | Sum | -19 | 22 | -30 | 1 | -27 | 55 | -71 | -103 | -2 | -121 |

Figures 2.2 ~ 2.9 provide the comparisons of the 51 and 252-group reactivity analysis results with the ENDF/B-7.0 and 7.1 cross-section libraries for the PWR and BWR fuel pin cell problems. Two different reactivity analyses have been carried out to see the reactivity changes due to either cross-section difference or cross-section plus scalar flux difference. The analysis results are almost similar with the 3-group analysis results, but more detailed information can be found as follows:

a. In 51-g structure U-235 1D cross sections of group-50 are wrong due to poor pointwise weighting function which requires more energy groups at this energy range.

b. In 51-g structure neutron spectrum of groups 42~51 are very poor resulting in significant reactivity differences which also requires energy group boundary refinement at this energy range.

c. In 51-g structure the quality of both 1D cross sections and scalar fluxes at groups 18 (30.0-48.0 eV), 19 (14.4-30.0 eV) and 23 (6.25-7.15 eV) are poor resulting in about 120 pcm difference. This means that energy group boundary is not good.

d. In 252-g structure the quality of both CENTRM-MOC and CENTRM-Sn cross sections are very good. However, some differences of 1D cross sections and scalar fluxes at groups 95 (101.2-105.0 eV), 103 (65.0-67.5 eV), 121 (36.0-37.0 eV) and 134 (20.5-21.2 eV) result in about 80 pcm reactivity differences.

e. In 252-g structure neutron spectra at groups 238~241 (0.03–0.055 eV) are poorly predicted resulting in relatively large reactivity biases for U-235 which may require more refined group structure at this energy range.

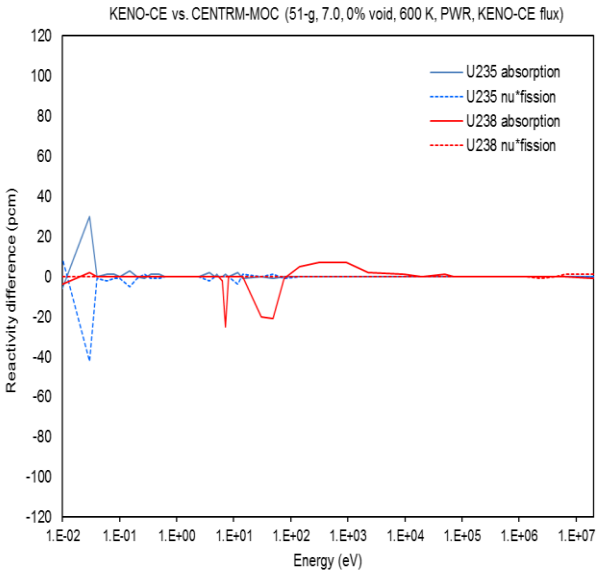


[CENTRM-MOC, XS effect]

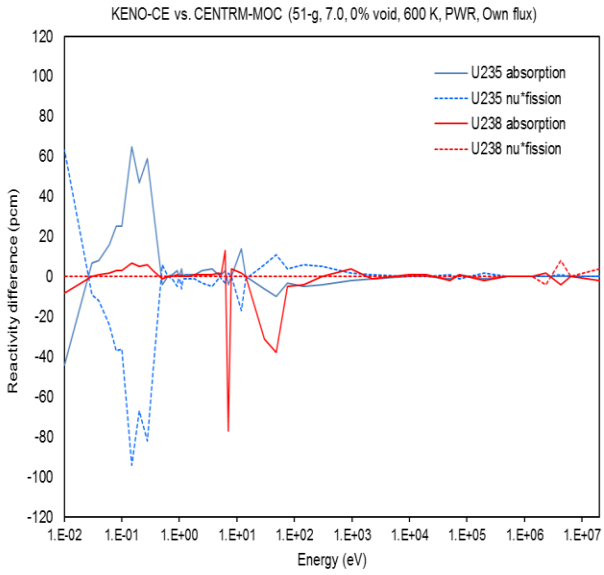


[CENTRM-MOC, XS/flux effect]

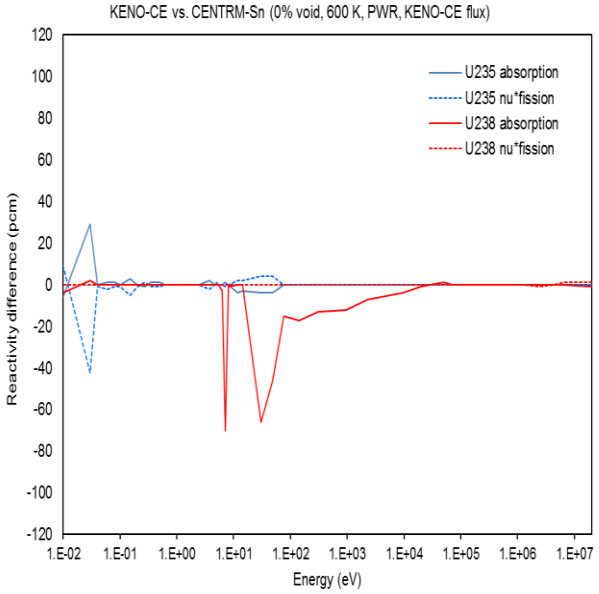


[CENTRM-Sn, XS effect]

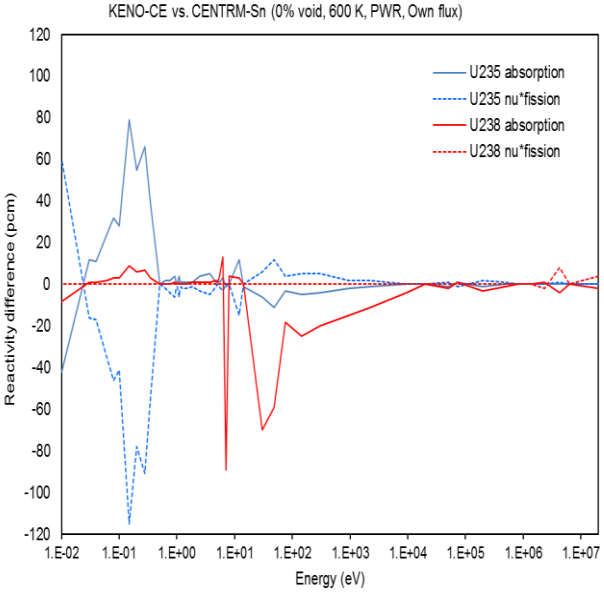


[CENTRM-Sn, XS/flux effect]

**Figure 2.2 Comparison of 51-group reactivity analysis (Case B, PWR, 600 K, ENDF/B-7.0)**

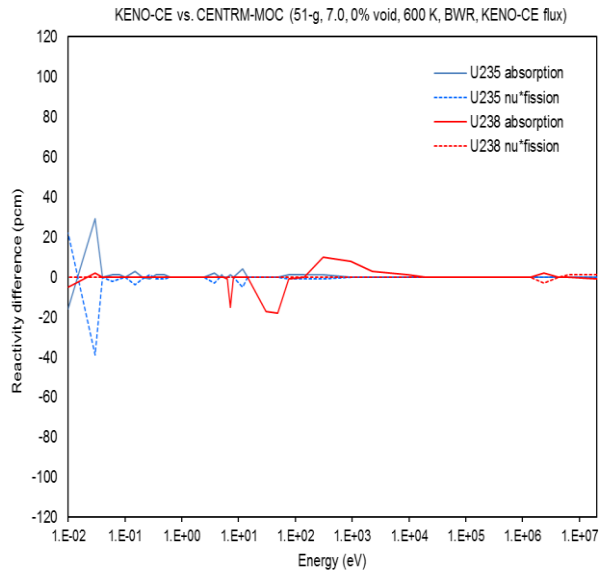


[CENTRM-MOC, XS effect]

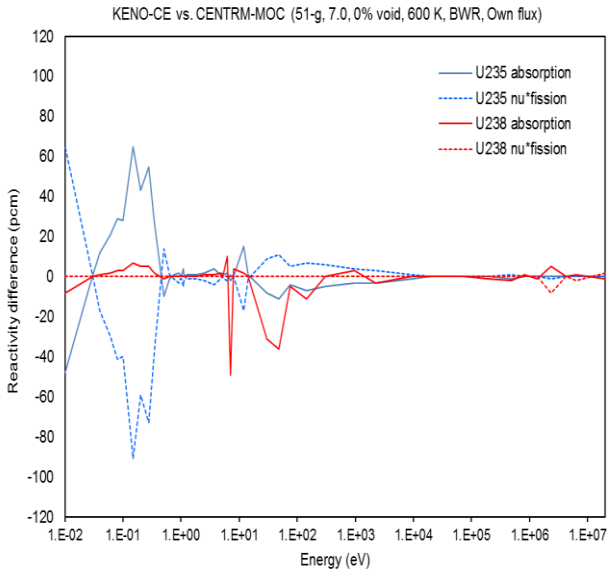


[CENTRM-MOC, XS/flux effect]

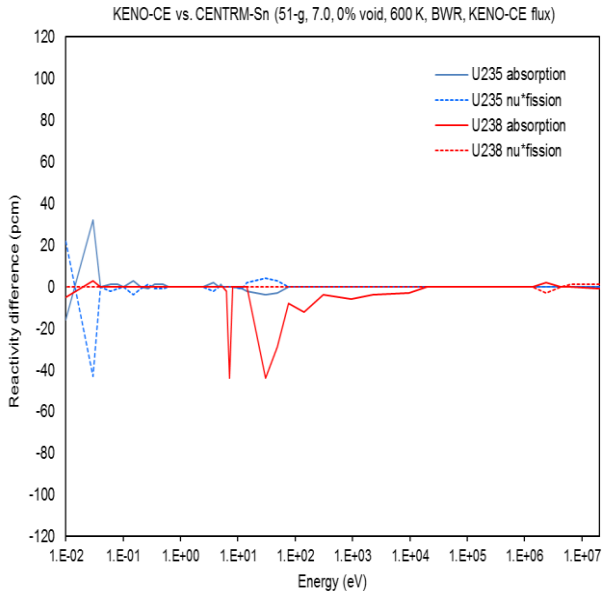


[CENTRM-Sn, XS effect]

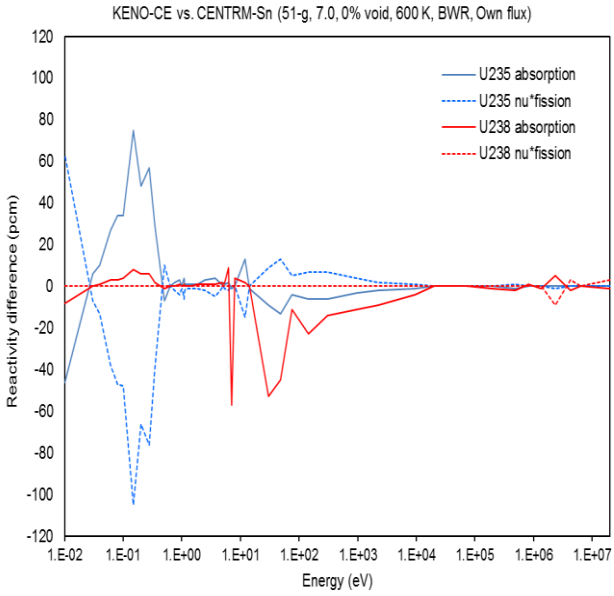


[CENTRM-Sn, XS/flux effect]

**Figure 2.3 Comparison of 51-group reactivity analysis (Case D, BWR, 600 K, ENDF/B-7.0)**

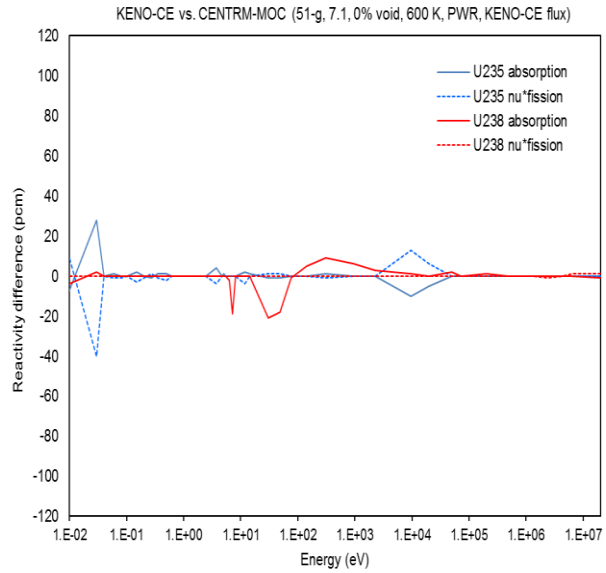


[CENTRM-MOC, XS effect]

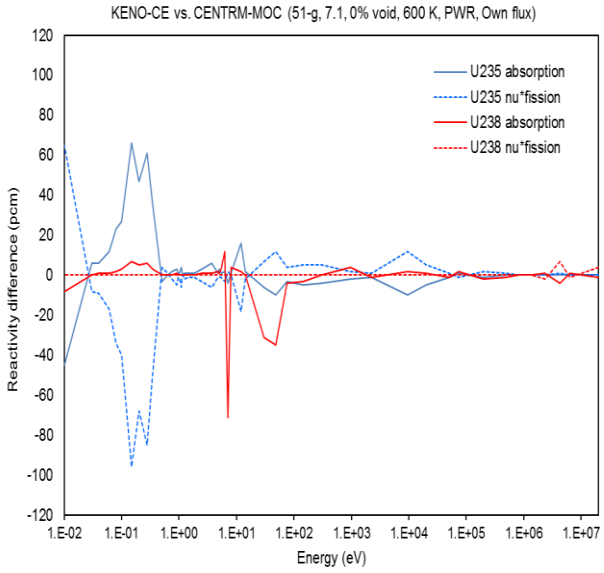


[CENTRM-MOC, XS/flux effect]

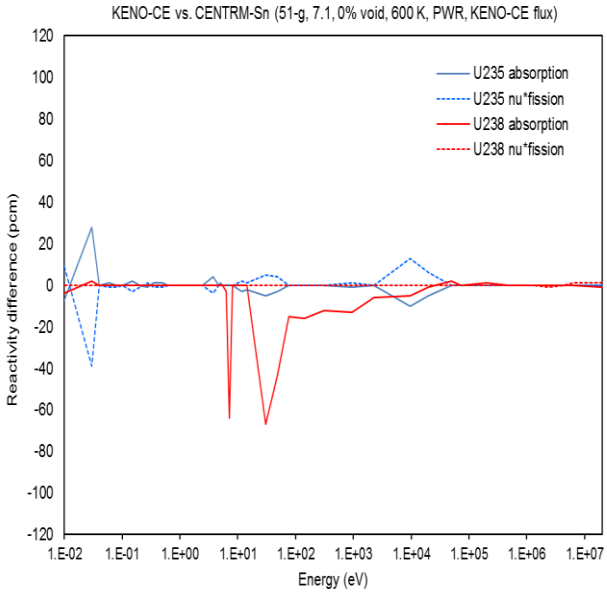


[CENTRM-Sn, XS effect]

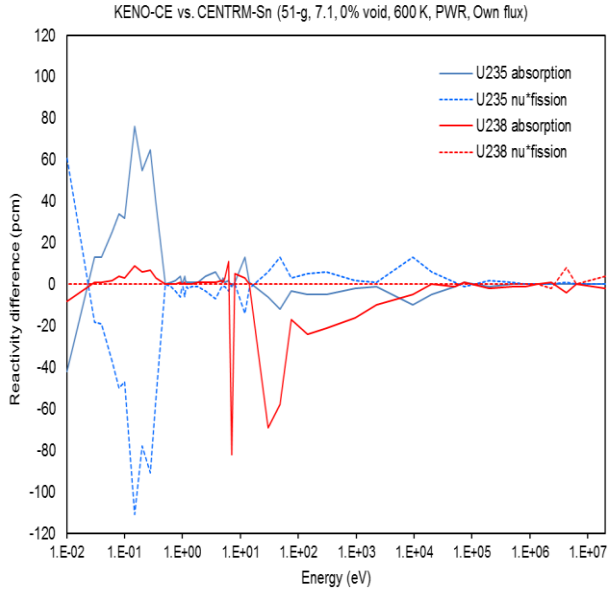


[CENTRM-Sn, XS/flux effect]

**Figure 2.4 Comparison of 51-group reactivity analysis (Case B, PWR, 600 K, ENDF/B-7.1)**

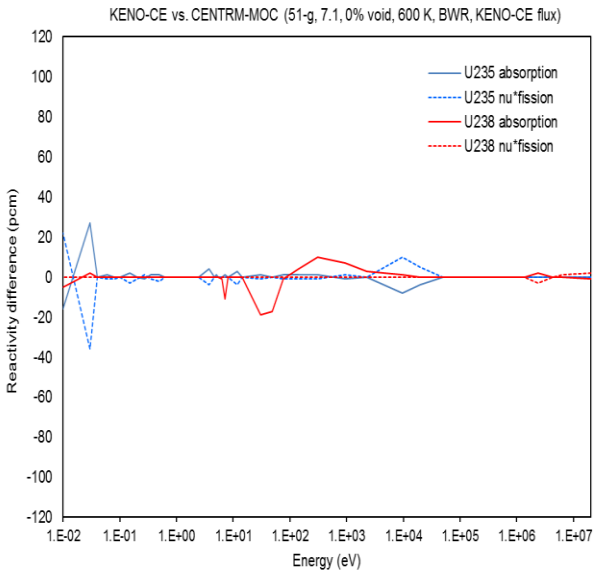


[CENTRM-MOC, XS effect]

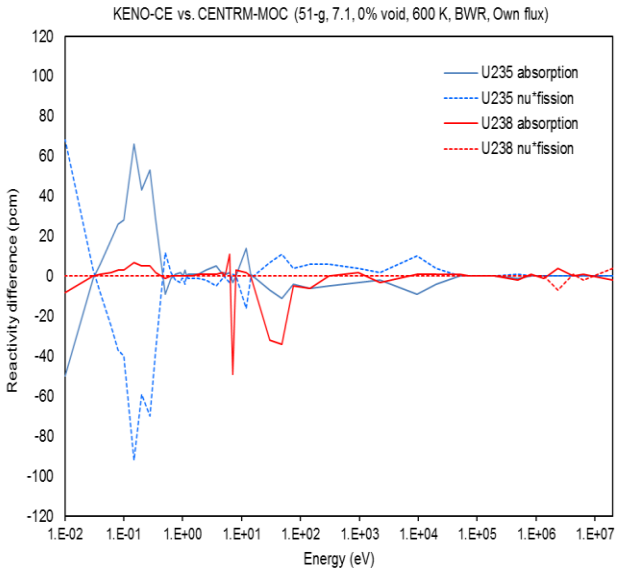


[CENTRM-MOC, XS/flux effect]

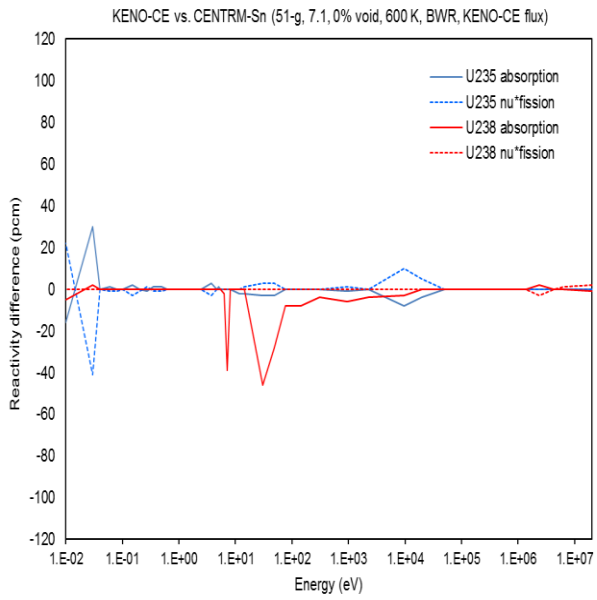


[CENTRM-Sn, XS effect]

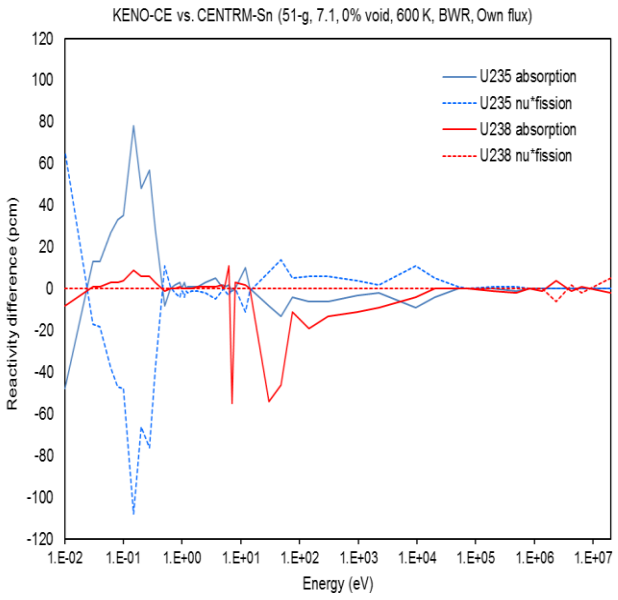


[CENTRM-Sn, XS/flux effect]

**Figure 2.5 Comparison of 51-group reactivity analysis (Case D, BWR, 600 K, ENDF/B-7.1)**

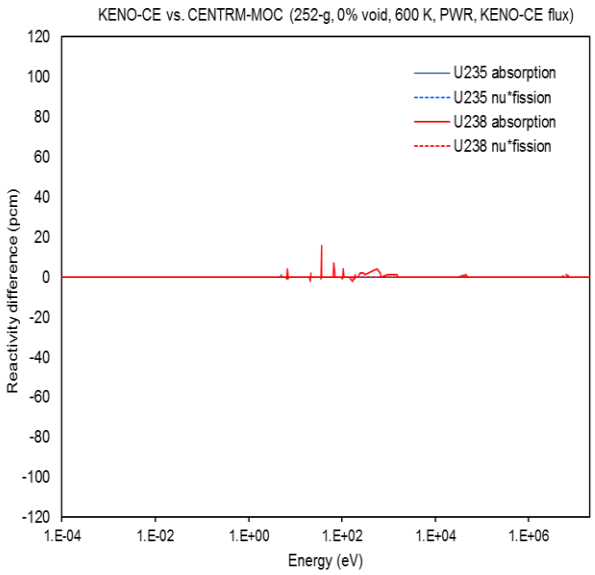


[CENTRM-MOC, XS effect]

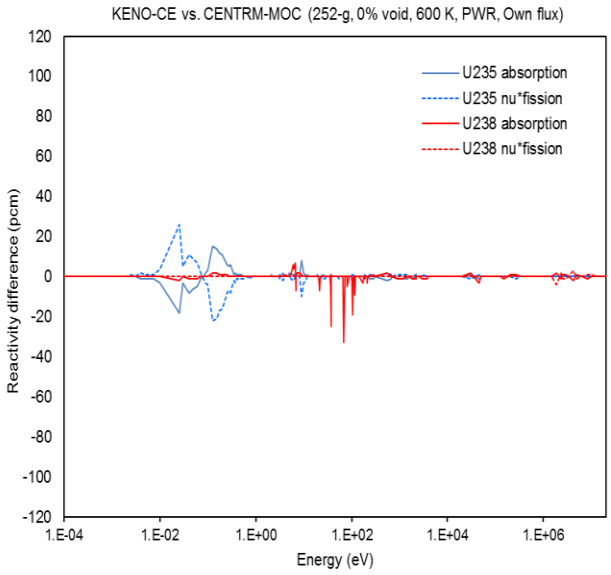


[CENTRM-MOC, XS/flux effect]

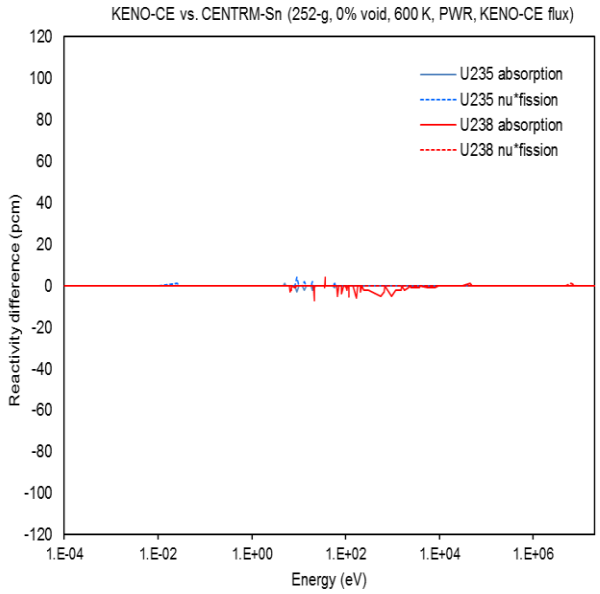


[CENTRM-Sn, XS effect]

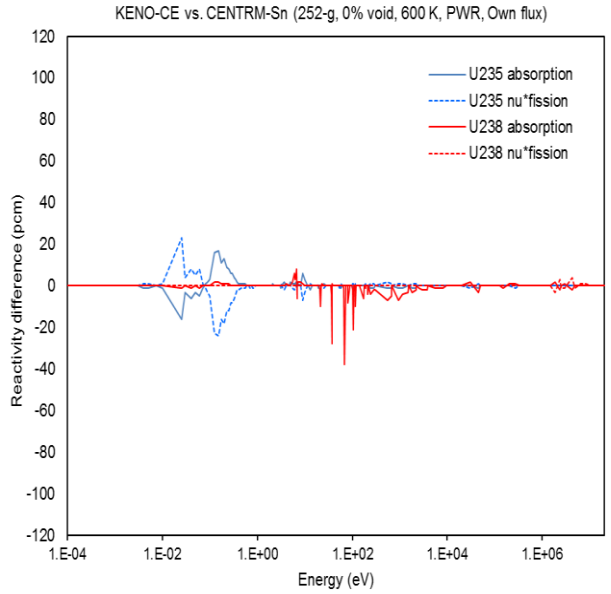


[CENTRM-Sn, XS/flux effect]

**Figure 2.6 Comparison of 252-group reactivity analysis (Case B, PWR, 600 K, ENDF/B-7.0)**

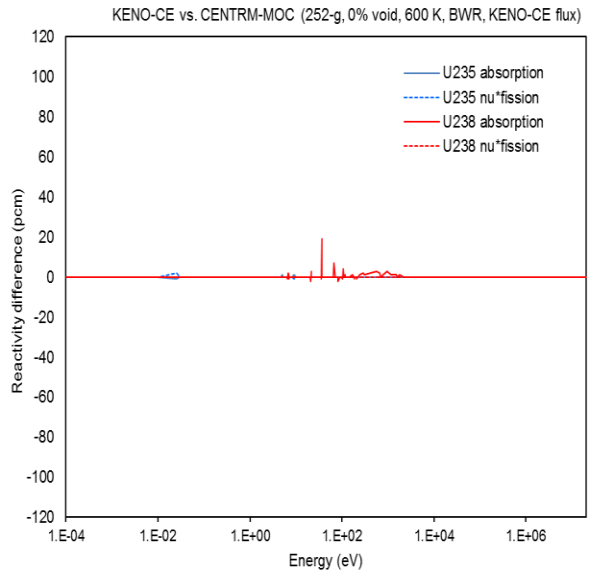


[CENTRM-MOC, XS effect]

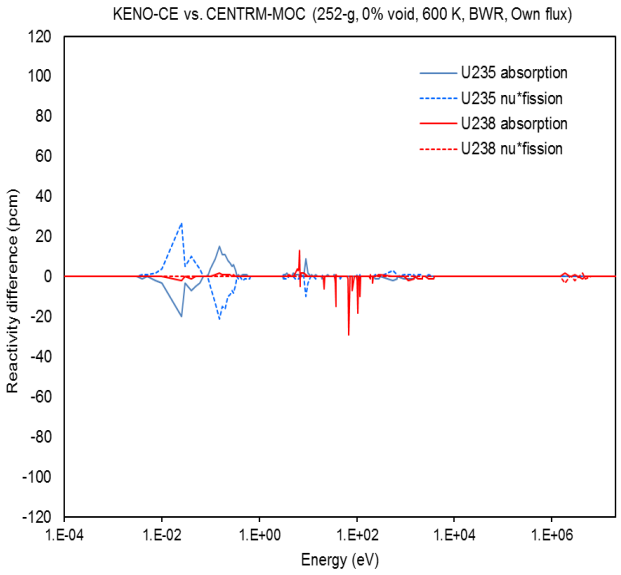


[CENTRM-MOC, XS/flux effect]

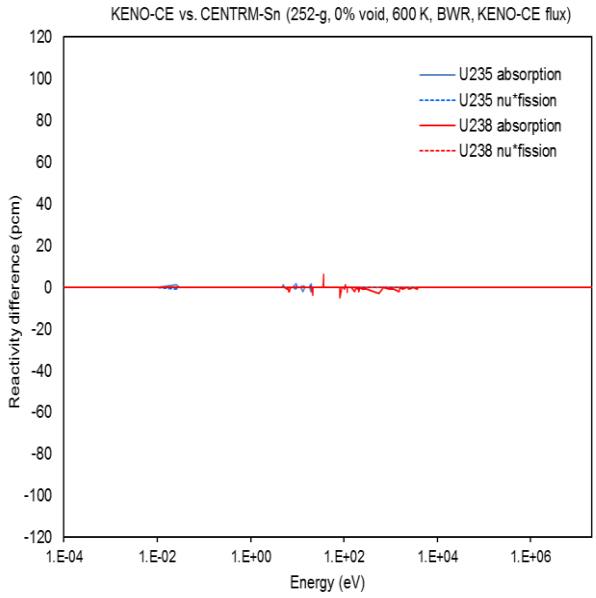


[CENTRM-Sn, XS effect]

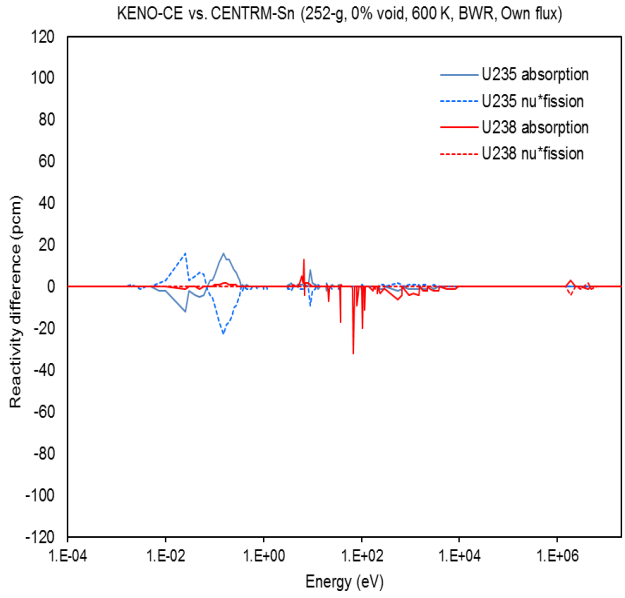


[CENTRM-Sn, XS/flux effect]

**Figure 2.7 Comparison of 252-group reactivity analysis (Case D, BWR, 600 K, ENDF/B-7.0)**

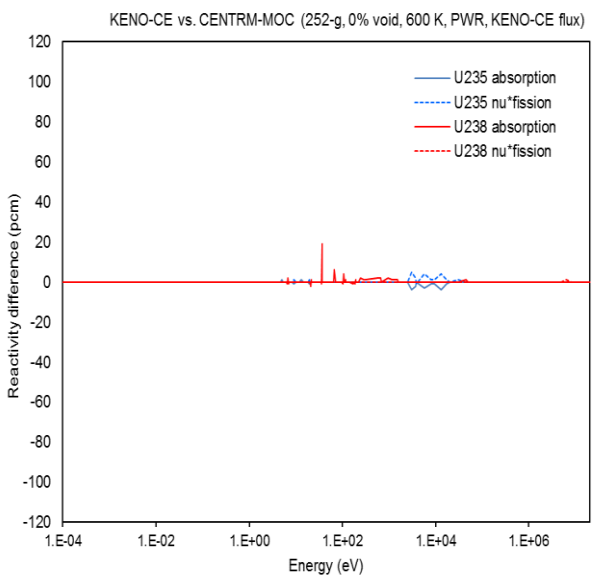


[CENTRM-MOC, XS effect]

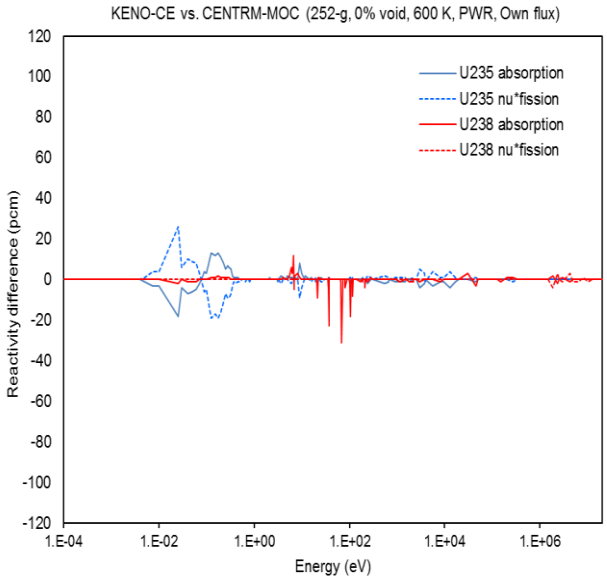


[CENTRM-MOC, XS/flux effect]

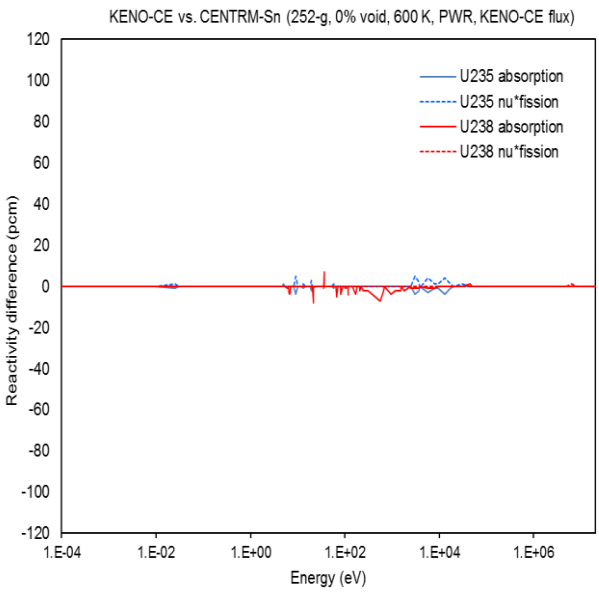


[CENTRM-Sn, XS effect]

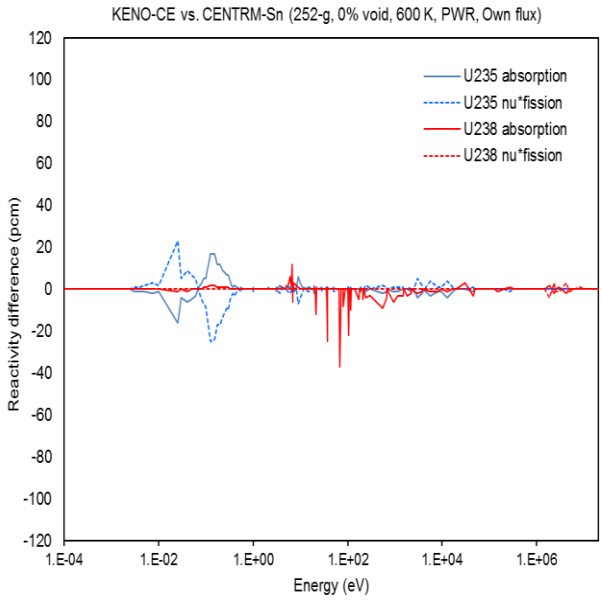


[CENTRM-Sn, XS/flux effect]

**Figure 2.8 Comparison of 252-group reactivity analysis (Case B, PWR, 600 K, ENDF/B-7.1)**

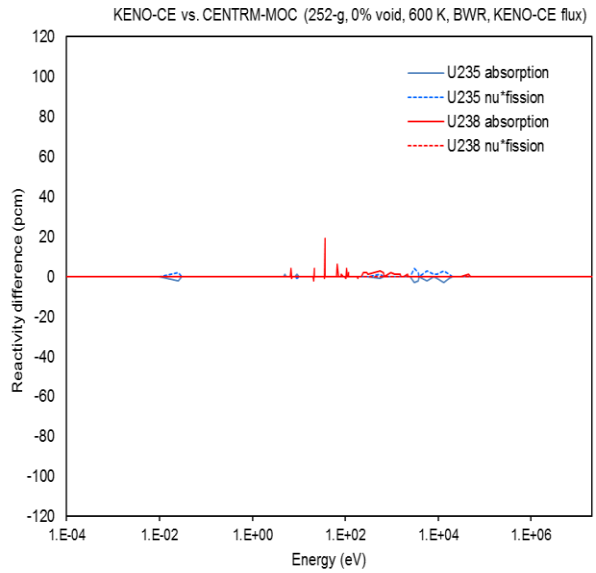


[CENTRM-MOC, XS effect]

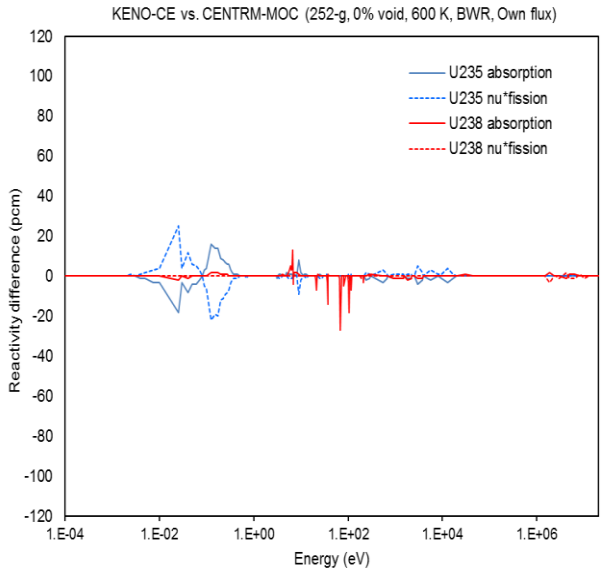


[CENTRM-MOC, XS/flux effect]

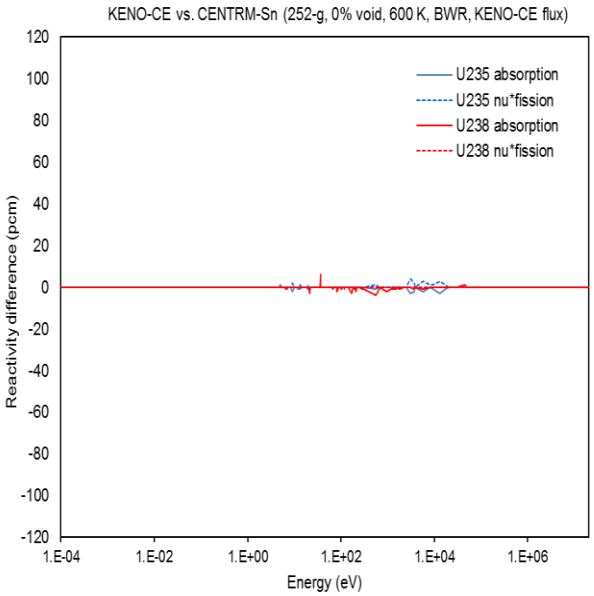


[CENTRM-Sn, XS effect]

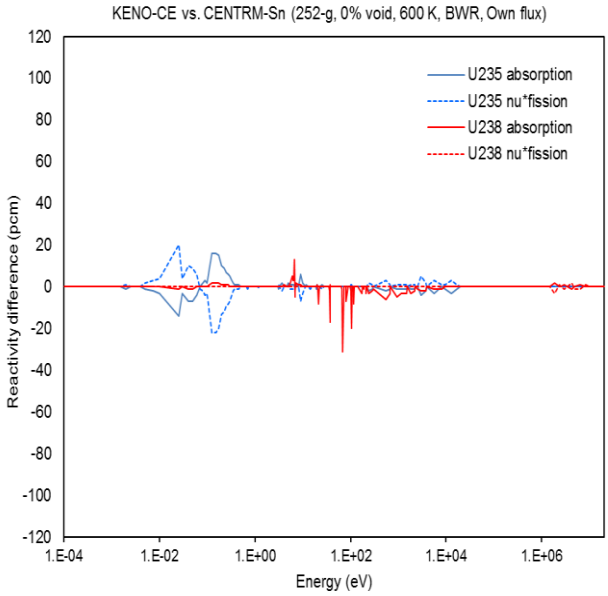


[CENTRM-Sn, XS/flux effect]

**Figure 2.9 Comparison of 252-group reactivity analysis (Case D, BWR, 600 K, ENDF/B-7.1)**

There have been significant improvements in CENTRM since SCALE-6.1. The followings are improvements.

a. Figure 2.10 provides a comparison of reactivity analysis between the old SCALE-6.1 238-group and the new 252-group CENTRM-MOC only due to the cross section differences for the same problem. Even though there are some differences in cross sections of CENTRM-MOC at low resolved resonance groups, there are significant improvements on thermal, high epithermal and fast energy groups. Some cross section differences at low U-238 resonances need to be improved which may be achieved by improving group structures.

b. Figure 2.11 provides a comparison of cross-section difference between CENTRM-MOC and KENO-CE for the old SCALE-6.1 238-g and new SCALE-6.3beta 252-group CENTRM calculations. There are significant improvements in 1D self-shielded cross sections.

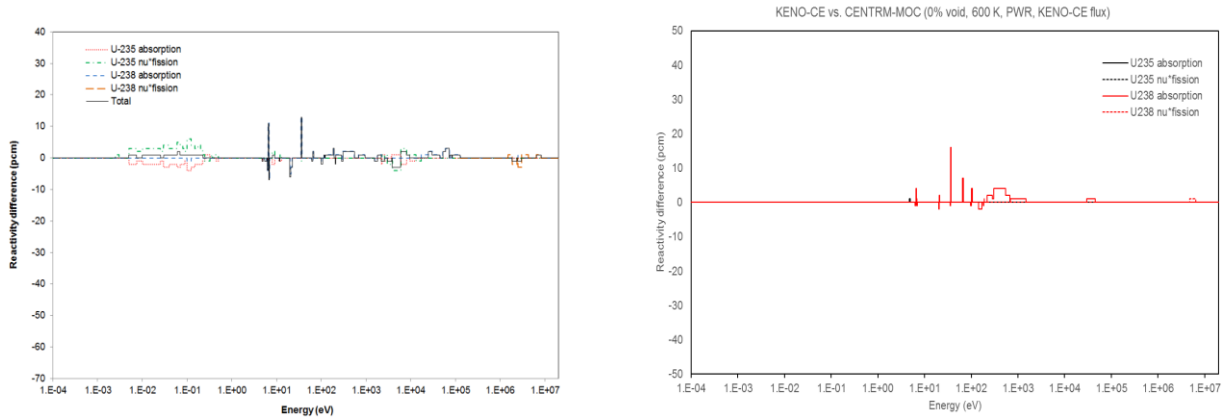


[Old MOC, 238-group] [New MOC, 252-group]

**Figure 2.10 Comparison of reactivity analysis (Old vs. New, Case B, PWR, 600 K, ENDF/B-7.0).**

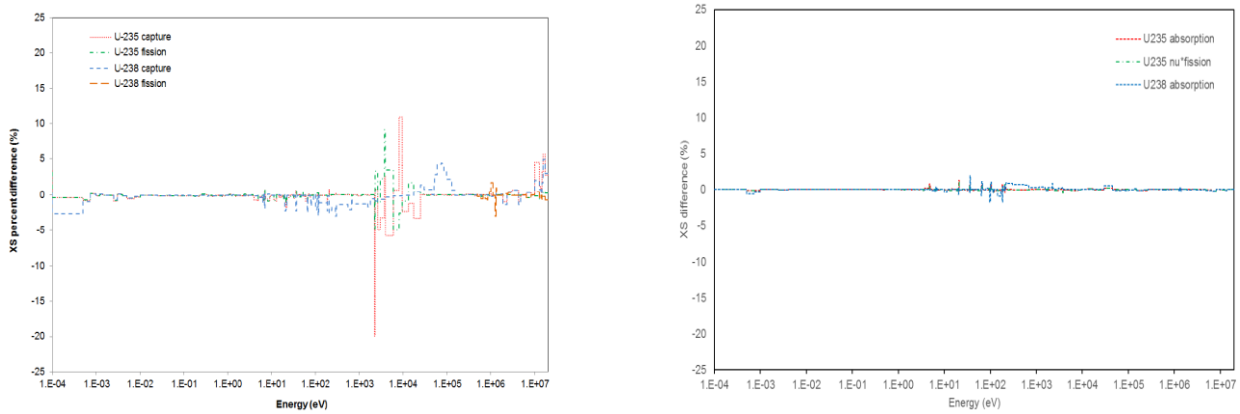


[Old MOC, 238-group] [New MOC, 252-group]

**Figure 2.11 Comparison of cross section differences (Old vs. New, Case B, PWR, 600 K, ENDF/B-7.0).**

# 3 SELF-SHIELDED CROSS-SECTION TABLESET GENERATION

Table 3.1 provides a sample of variations to achieve various background cross sections in heterogeneous models by changing moderator and fuel compositions and geometrical configurations. Assessment has been performed by comparing the self-shielded cross-section tables generated by IRFFACTOR with those by another program, MERIT.

Figures 4.1 to 4.4 provide comparisons of absorption self-shielded cross-section tables for important resonance group-21 and -23 of $^{235}U$ and group-23 of $^{238}U$ at 51-group structure in which they are very consistent with each other.

**Table 3.1. Variations of composition and geometry for heterogeneous F-factors**

| Case | Fuel | | | Clad | $H_2O$ | | Radius or Pitch (cm) | | |
|---|---|---|---|---|---|---|---|---|---|
| | $^{235}U$ | $^{238}U$ | $^{16}O$ | $^{27}Al$ | $^{1}H$ | $^{16}O$ | Fuel | Clad | Pitch |
| 1 | 9.39467E-04 | 2.22624E-02 | 4.64223E-02 | 6.02611E-02 | 1.17827E-04 | 5.89135E-05 | 0.4025 | 0.4759 | 1.2620 |
| 2 | 9.39467E-04 | 2.22624E-02 | 4.64223E-02 | 6.02611E-02 | 9.42618E-03 | 4.71308E-03 | 0.4025 | 0.4759 | 1.2620 |
| 3 | 9.39467E-04 | 2.22624E-02 | 4.64223E-02 | 6.02611E-02 | 2.35655E-02 | 1.17827E-02 | 0.4025 | 0.4759 | 1.2620 |
| 4 | 9.39467E-04 | 2.22624E-02 | 4.64223E-02 | 6.02611E-02 | 3.53482E-02 | 1.76741E-02 | 0.4025 | 0.4759 | 1.2620 |
| 5 | 9.39467E-04 | 2.22624E-02 | 4.64223E-02 | 6.02611E-02 | 4.71309E-02 | 2.35654E-02 | 0.4025 | 0.4759 | 1.2620 |
| 6 | 9.39467E-04 | 2.22624E-02 | 4.64223E-02 | 6.02611E-02 | 4.71309E-02 | 2.35654E-02 | 0.4025 | 0.4759 | 1.5728 |
| 7 | 9.39467E-04 | 2.22624E-02 | 4.64223E-02 | 6.02611E-02 | 4.71309E-02 | 2.35654E-02 | 0.4025 | 0.4759 | 2.2620 |
| 8 | 4.69734E-04 | 1.11312E-02 | 2.32112E-02 | 6.02611E-02 | 4.71309E-02 | 2.35654E-02 | 0.4025 | 0.4759 | 2.2620 |
| 9 | 2.34867E-04 | 5.56560E-03 | 1.16056E-02 | 6.02611E-02 | 4.71309E-02 | 2.35654E-02 | 0.4025 | 0.4759 | 2.2620 |
| 10 | 1.17433E-04 | 2.78280E-03 | 5.80279E-03 | 6.02611E-02 | 4.71309E-02 | 2.35654E-02 | 0.4025 | 0.4759 | 2.2620 |
| 11 | 5.87167E-05 | 1.39140E-03 | 2.90139E-03 | 6.02611E-02 | 4.71309E-02 | 2.35654E-02 | 0.4025 | 0.4759 | 2.2620 |
| 12 | 2.93583E-05 | 6.95700E-04 | 1.45070E-03 | 6.02611E-02 | 4.71309E-02 | 2.35654E-02 | 0.4025 | 0.4759 | 2.2620 |
| 13 | 9.39467E-06 | 2.22624E-04 | 4.64223E-04 | 6.02611E-02 | 4.71309E-02 | 2.35654E-02 | 0.4025 | 0.4759 | 2.2620 |
| 14 | 9.39467E-06 | 2.22624E-05 | 4.64223E-04 | 6.02611E-02 | 4.71309E-02 | 2.35654E-02 | 0.4025 | 0.4759 | 2.2620 |
| 15 | 9.39467E-06 | 2.22624E-08 | 4.64223E-04 | 6.02611E-02 | 4.71309E-02 | 2.35654E-02 | 0.4025 | 0.4759 | 2.2620 |
| 16 | 9.39467E-06 | 2.22624E-09 | 4.64223E-04 | 6.02611E-02 | 4.71309E-02 | 2.35654E-02 | 0.4025 | 0.4759 | 2.2620 |

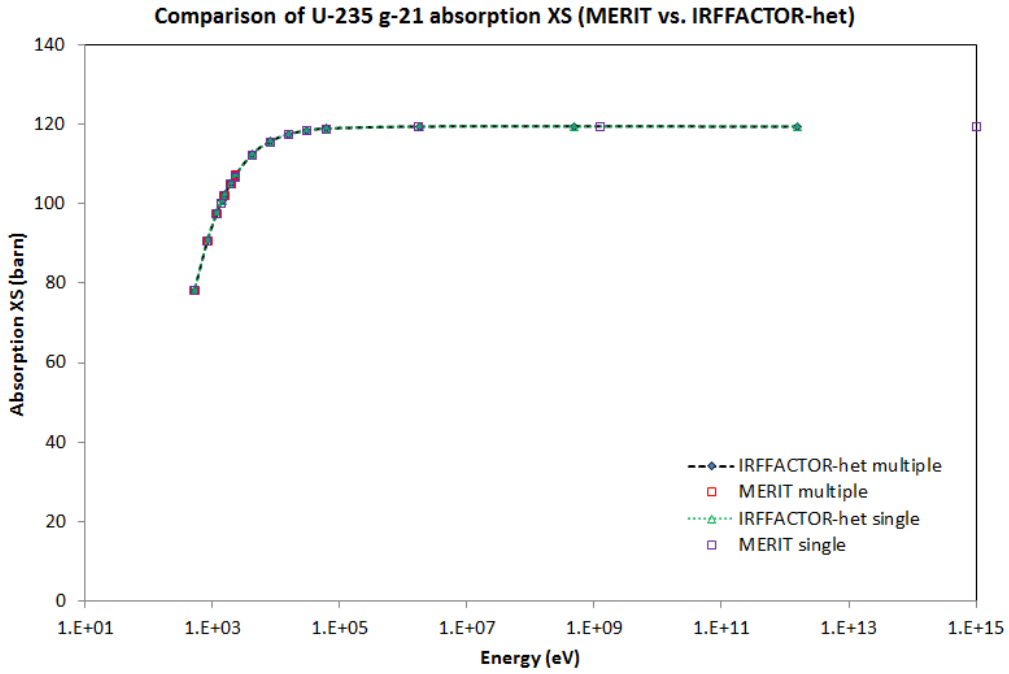


**Figure 3.1 Comparison of self-shielded XS tables for $^{235}$U group-21 absorption.**

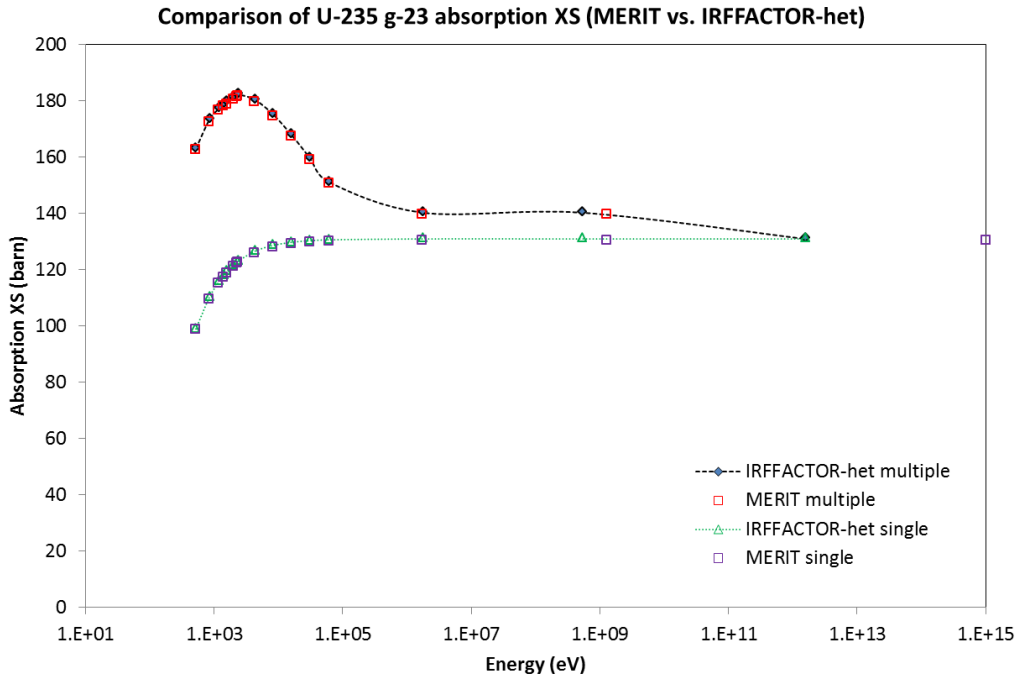


**Figure 3.2 Comparison of self-shielded XS tables for $^{235}$U group-23 absorption.**

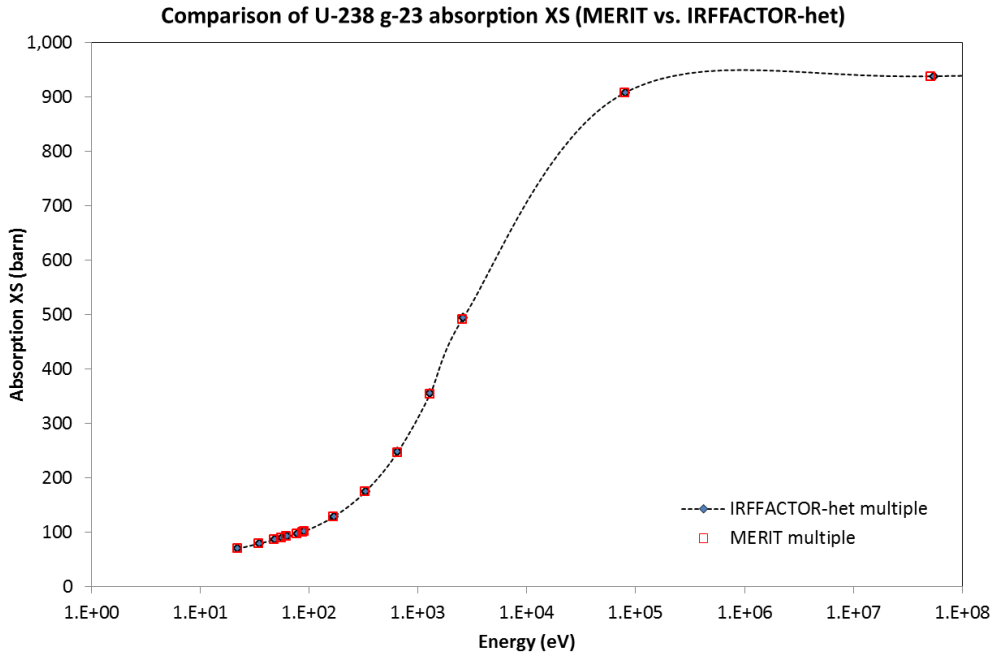


**Figure 3.3 Comparison of self-shielded XS tables for $^{238}$U group-23 absorption (Multiple absorber model).**

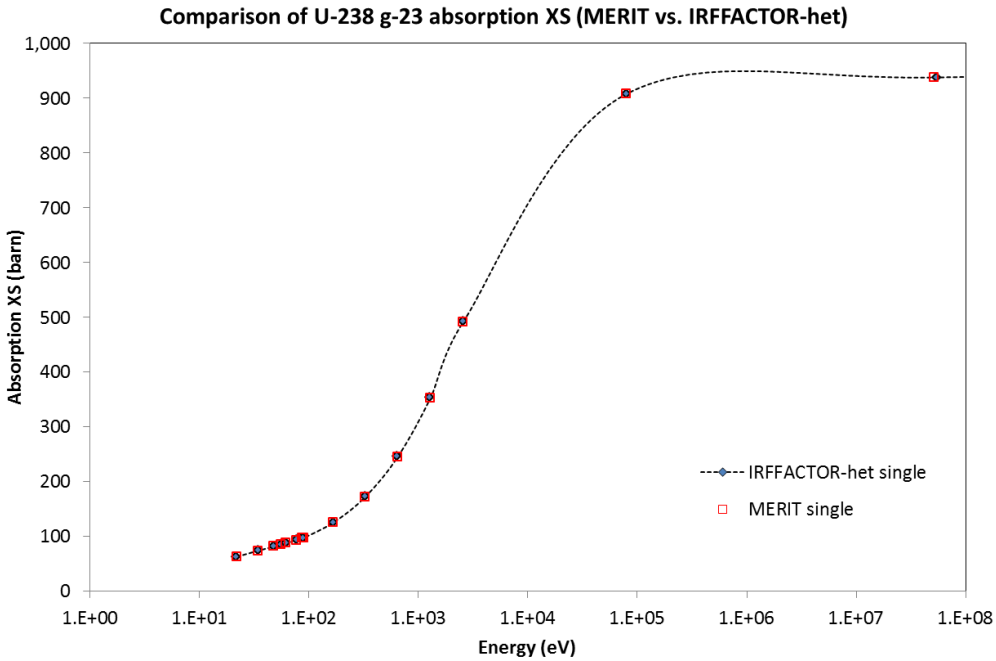


**Figure 3.4 Comparison of self-shielded XS tables for $^{238}$U group-23 absorption (Single absorber model).**

# 4 SUBGROUP DATA GENERATION AND RECONSTRUCTION

The SUBGR program internally includes a verification procedure by comparing the reconstructed RIs or XSs from subgroup data to the original RIs or XSs. Therefore, verification for the subgroup data generation does not need to be discussed in this document. However, it is required to review if the MPACT subgroup module is able to correctly estimate self-shield cross sections to be consistent with the original resonance self-shielded cross-section data.

The MPACT subgroup module includes a Bondarenko iteration to consider resonance interferences between resonance nuclides. Since typically resonance self-shielded cross-section tables are generated excluding resonance interferences, the Bondarenko iteration needs to be skipped for this assessment. Since the MPACT does not include the user option, the MPACT has been modified to skip the Bondarenko iteration only for this verification process.

In Table 3.1 the variation case-5 has been selected for this assessment. Absorption and $\nu$*fission self-shielded cross sections for $^{235}$U and $^{238}$U have been estimated by the MPACT subgroup calculations without considering resonance interferences. Figures 4.1 to 4.3 provide comparisons of self-shielded cross sections between MPACT and IRFFACTOR which are very consistent with each other.

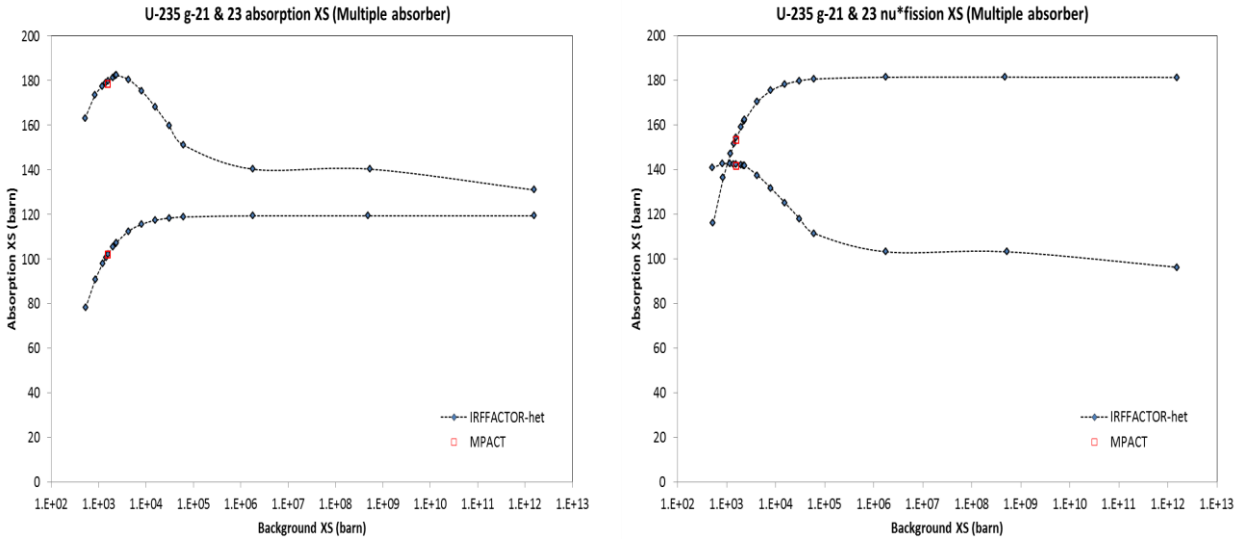


**Figure 4.1 Reconstruction of the self-shielded cross sections by MPACT ($^{235}$U groups-21 and -23, absorption and $\nu$*fission, multiple absorber model).**

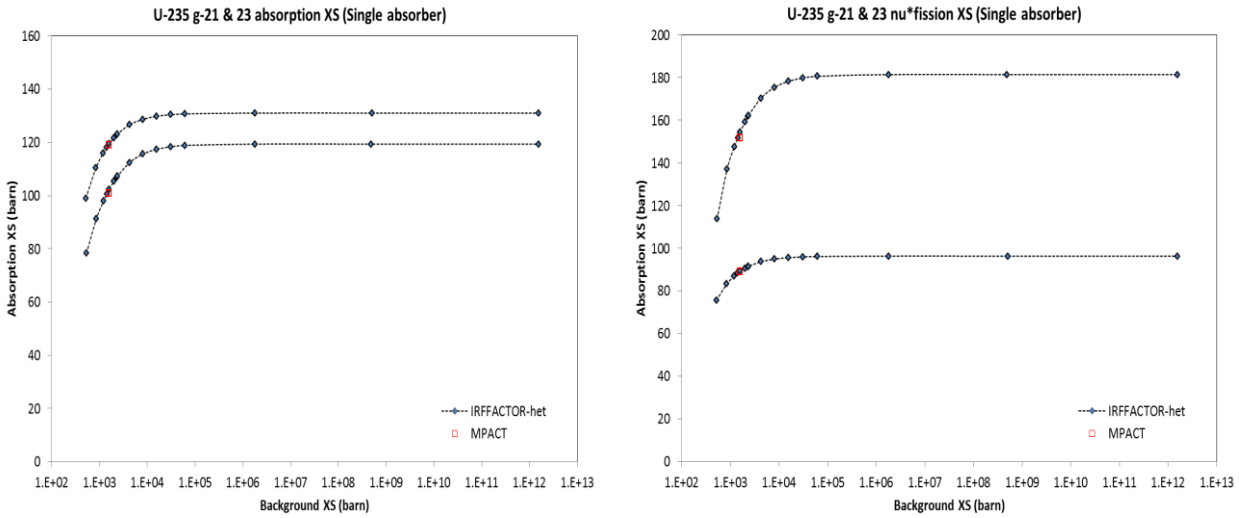


**Figure 4.2 Reconstruction of the self-shielded cross sections by MPACT ($^{235}$U groups-21 and -23, absorption and ν*fission, single absorber model).**

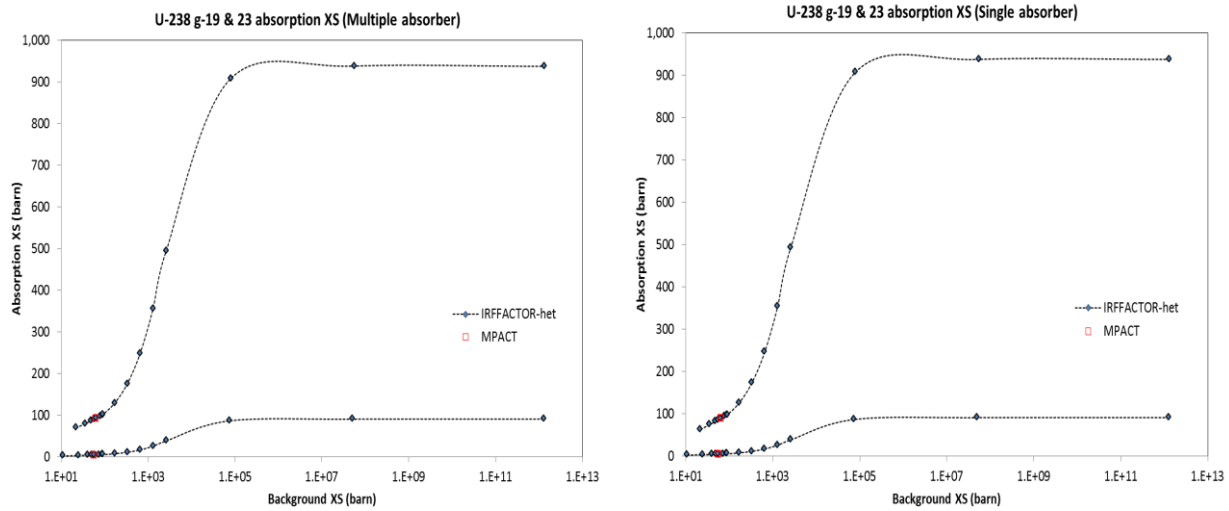


**Figure 4.3 Reconstruction of the self-shielded cross sections by MPACT ($^{238}$U groups-19 and -23, absorption, single/multiple absorber models).**

# 5 CONCLUSION

Intensive investigation has been performed to determine whether the current CENTRM-MOC is working correctly. It is noted that the current CENTRM-MOC is working correctly. However, it should be noted that there are still non-negligible errors in predicting self-shielded cross sections for some of the $^{238}U$ large resonances which can be converted into about 10-20-pcm reactivity error for each resonance in 252-group structure. The total reactivity by CENTRM-MOC is underestimated by about 100 pcm, which needs to be improved. The 51-group structure is not best optimized resulting in temperature reactivity bias and larger reactivity differences compared to the 252-group results. Therefore, the 51-g structure needs to be improved to resolve the temperature reactivity bias and $k_{eff}$'s.

Self-shielded cross section tables generated by IRFFACTOR with heterogeneous models are very consistent with those by the other slowing down program called MERIT, employing the same ESSM calculation to obtain background cross sections. Note that the AMPX self-shielded cross section tables are being correctly generated by the SCALE/AMPX IRFFACTOR.

Note that self-shielded cross sections estimated by the MPACT subgroup module are very consistent with the original self-shielded cross-section tables prepared by IRFFACTOR, which indicates that the MPACT subgroup module is working correctly.

## REFERENCES

[Kim12] Kang Seog Kim, Mark L. Williams, “The Method of Characteristics For 2-D Multigroup and Pointwise Transport Calculation in SCALE/CENTRM,” PHYSOR 2012, Knoxville, Tennessee, USA, April 15-20, 2012 (2012).

[Kim16a] Kang Seog Kim, “SUBGR: A Program to Generate Subgroup Data for the Subgroup Resonance Self-Shielding Calculation,” CASL-U-2016-1071-000, ORNL/TM-2016/154 (2016).

[Kim16b] Kang Seog Kim, “Generation of the V4.2m1 AMPX and MPACT 51 and 252-group Libraries with ENDF/B-VII.0 and ENDF/B-VII.1,” CASL-U-2016-1177-000, ORNL/TM-2016/555 (2016).

[Rea16] Rearden, B. T. and M. A. Jessee, “SCALE Code System,” ORNL/TM-2005/39, Version 6.2 (2016).

[Wia16] Wiarda, D. et al., “AMPX-6: A Modular Code System for Processing ENDF/B Evaluations,” ORNL/TM-2016/43 (2016).

[Wil06] Mark L. Williams, M. Asgari, D. F. Hollenbach, *CENTRM: A One-Dimensional Neutron Transport Code For Computing Pointwise Energy Spectra*, ORNL/TM-2005/39, Version 5.1, Vol. II, Book 4, Sect. F18 (2006).

[Wil12] Mark L. Williams and Kang-Seog Kim, “The Embedded Self-Shielding Method,” PHYSOR 2012, Knoxville, Tennessee, USA (2012).

# APPENDIX A1. SAMPLE INPUT OF KENO-CE WITH ENDF/B-7.0

```
=csas6
centrm verification pincell c01 00.00 % void 293.6 K
ce_v7.0_endf
read comp
' Fuel
u-235 1 0  9.39467E-4 293.6  end
u-238 1 0  2.22624E-2 293.6  end
o-16  1 0  4.64223E-2 293.6  end
' Clad
al-27 2 0  6.02611E-2 293.6 end
' h2o
h-1   3 0  6.72142E-2 293.6  end
o-16  3 0  3.36071E-2 293.6  end
end comp

read parm
  gen=200 npg=200000 nsk=100  scx=no
end parm

read geom
global unit 10
cylinder 11 0.4025 chord +x=0.0 chord +y=0.0
cylinder 12 0.4759 chord +x=0.0 chord +y=0.0
cuboid 13 0.6310 0.0 0.6310 0.0 5.0 -5.0
media 1 1 11
media 2 1 12 -11
media 3 1 13 -12
boundary 13
end geom

read bounds
all=refl
end bounds

read reactions
   xs=yes rx=yes unit=3
   mix=1
   nuclist 92238 92235 end
   mtlist 102 18 2 end
end reactions

read energy
 2.00000E+07 1.73300E+07 1.56800E+07 1.45500E+07 1.38400E+07
 1.28400E+07 1.00000E+07 8.18700E+06 6.43400E+06 4.80000E+06
 4.30400E+06 3.00000E+06 2.47900E+06 2.35400E+06 1.85000E+06
 1.50000E+06 1.40000E+06 1.35600E+06 1.31700E+06 1.25000E+06
 1.20000E+06 1.10000E+06 1.01000E+06 9.20000E+05 9.00000E+05
 8.75000E+05 8.61100E+05 8.20000E+05 7.50000E+05 6.79000E+05
 6.70000E+05 6.00000E+05 5.73000E+05 5.50000E+05 4.92000E+05
 4.70000E+05 4.40000E+05 4.20000E+05 4.00000E+05 3.30000E+05
 2.70000E+05 2.00000E+05 1.49000E+05 1.28300E+05 1.00000E+05
 8.50000E+04 8.20000E+04 7.50000E+04 7.30000E+04 6.00000E+04
 5.20000E+04 5.00000E+04 4.50000E+04 3.00000E+04 2.50000E+04
 1.70000E+04 1.30000E+04 9.50000E+03 8.03000E+03 6.00000E+03
 3.90000E+03 3.74000E+03 3.00000E+03 2.58000E+03 2.29000E+03
 2.20000E+03 1.80000E+03 1.55000E+03 1.50000E+03 1.15000E+03
 9.50000E+02 6.83000E+02 6.70000E+02 5.50000E+02 3.05000E+02
 2.85000E+02 2.40000E+02 2.20000E+02 2.09500E+02 2.07400E+02
 2.02000E+02 1.93000E+02 1.91500E+02 1.88500E+02 1.87700E+02
 1.80000E+02 1.70000E+02 1.43000E+02 1.22000E+02 1.19000E+02
 1.17500E+02 1.16000E+02 1.13000E+02 1.08000E+02 1.05000E+02
 1.01200E+02 9.70000E+01 9.00000E+01 8.17000E+01 8.00000E+01
 7.60000E+01 7.20000E+01 6.75000E+01 6.50000E+01 6.30000E+01
```

```
 6.10000E+01 5.80000E+01 5.34000E+01 5.06000E+01 4.83000E+01
 4.52000E+01 4.40000E+01 4.24000E+01 4.10000E+01 3.96000E+01
 3.91000E+01 3.80000E+01 3.76300E+01 3.72700E+01 3.71300E+01
 3.70000E+01 3.60000E+01 3.55000E+01 3.50000E+01 3.37500E+01
 3.32500E+01 3.17500E+01 3.12500E+01 3.00000E+01 2.75000E+01
 2.50000E+01 2.25000E+01 2.17500E+01 2.12000E+01 2.05000E+01
 2.00000E+01 1.94000E+01 1.85000E+01 1.70000E+01 1.60000E+01
 1.44000E+01 1.29000E+01 1.19000E+01 1.15000E+01 1.00000E+01
 9.10000E+00 8.10000E+00 7.15000E+00 7.00000E+00 6.87500E+00
 6.75000E+00 6.50000E+00 6.25000E+00 6.00000E+00 5.40000E+00
 5.00000E+00 4.70000E+00 4.10000E+00 3.73000E+00 3.50000E+00
 3.20000E+00 3.10000E+00 3.00000E+00 2.97000E+00 2.87000E+00
 2.77000E+00 2.67000E+00 2.57000E+00 2.47000E+00 2.38000E+00
 2.30000E+00 2.21000E+00 2.12000E+00 2.00000E+00 1.94000E+00
 1.86000E+00 1.77000E+00 1.68000E+00 1.59000E+00 1.50000E+00
 1.45000E+00 1.40000E+00 1.35000E+00 1.30000E+00 1.25000E+00
 1.22500E+00 1.20000E+00 1.17500E+00 1.15000E+00 1.14000E+00
 1.13000E+00 1.12000E+00 1.11000E+00 1.10000E+00 1.09000E+00
 1.08000E+00 1.07000E+00 1.06000E+00 1.05000E+00 1.04000E+00
 1.03000E+00 1.02000E+00 1.01000E+00 1.00000E+00 9.75000E-01
 9.50000E-01 9.25000E-01 9.00000E-01 8.50000E-01 8.00000E-01
 7.50000E-01 7.00000E-01 6.50000E-01 6.25000E-01 6.00000E-01
 5.50000E-01 5.00000E-01 4.50000E-01 4.00000E-01 3.75000E-01
 3.50000E-01 3.25000E-01 3.00000E-01 2.75000E-01 2.50000E-01
 2.25000E-01 2.00000E-01 1.75000E-01 1.50000E-01 1.25000E-01
 1.00000E-01 9.00000E-02 8.00000E-02 7.00000E-02 6.00000E-02
 5.00000E-02 4.00000E-02 3.00000E-02 2.53000E-02 1.00000E-02
 7.50000E-03 5.00000E-03 4.00000E-03 3.00000E-03 2.50000E-03
 2.00000E-03 1.50000E-03 1.20000E-03 1.00000E-03 7.50000E-04
 5.00000E-04 1.00000E-04 1.00000E-05
end energy

end data
end
```

# APPENDIX A2. SAMPLE INPUT OF CENTRM-MOC + KENO-MG

```
=shell
ln -sf /home/ykk/URR/scale.rev01.xn252v7  ft99f001
end
=csas6 parm=(centrm)
centrm verification pincell c01 00.00 % void 293.6 K
ft99f001
read comp
' Fuel
u-235 1 0  9.39467E-4 293.6  end
u-238 1 0  2.22624E-2 293.6  end
o-16  1 0  4.64223E-2 293.6  end
' Clad
al-27 2 0  6.02611E-2 293.6 end
' h2o
h-1   3 0  6.72142E-2 293.6  end
o-16  3 0  3.36071E-2 293.6  end
end comp

read celldata
 latticecell squarepitch   pitch=1.2620 3 fueld=0.8050 1 cladd=0.9518  2  end
 centrmdata  iup=20 iprt=-1 nprt=2 npxs=6  mocMesh=1  end centrmdata
end celldata

read parm
  gen=200 npg=400000 nsk=100 flx=yes
end parm

read geom
global unit 10
cylinder 11 0.4025 chord +x=0.0 chord +y=0.0
cylinder 12 0.4759 chord +x=0.0 chord +y=0.0
cuboid 13 0.6310 0.0 0.6310 0.0 5.0 -5.0
media 1 1 11
media 2 1 12 -11
media 3 1 13 -12
boundary 13
end geom

read bounds
all=refl
end bounds

end data
end
```

# APPENDIX A3. SAMPLE INPUT OF CENTRM-SN + KENO-MG

```
=shell
ln -sf /home/ykk/URR/scale.rev01.xn252v7  ft99f001
end
=csas6 parm=(centrm)
centrm verification pincell c01 00.00 % void 293.6 K
ft99f001
read comp
' Fuel
u-235 1 0  9.39467E-4 293.6  end
u-238 1 0  2.22624E-2 293.6  end
o-16  1 0  4.64223E-2 293.6  end
' Clad
al-27 2 0  6.02611E-2 293.6 end
' h2o
h-1   3 0  6.72142E-2 293.6  end
o-16  3 0  3.36071E-2 293.6  end
end comp

read celldata
 latticecell squarepitch   pitch=1.2620 3 fueld=0.8050 1 cladd=0.9518  2  end
 centrmdata  iup=20 iprt=-1 nprt=2 npxs=1  end centrmdata
end celldata

read parm
  gen=200 npg=400000 nsk=100 flx=yes
end parm

read geom
global unit 10
cylinder 11 0.4025 chord +x=0.0 chord +y=0.0
cylinder 12 0.4759 chord +x=0.0 chord +y=0.0
cuboid 13 0.6310 0.0 0.6310 0.0 5.0 -5.0
media 1 1 11
media 2 1 12 -11
media 3 1 13 -12
boundary 13
end geom

read bounds
all=refl
end bounds

end data
end
```

# APPENDIX B1. SAMPLE INPUT OF IRFFACTOR-HET

```
' ------------------------------------------------------------------------------
' Heterogeneous irffactor for U-238 :: multiple absorber ENDF/B-VII.0
' ------------------------------------------------------------------------------
=shell
ln -sf $RTNDIR/../cases/U238-HetCases-new.inp het_input
ln -sf /home/ykk/libraries/endf7.0/mg/51g19g2new/ampx51g_70_test_01.bin  ft88f001
ln -sf /home/xmw/S/build/gnu-RELEASE/INSTALL/bin/irffactor irffactor
ln -sf /home/xmw/S/build/gnu-RELEASE/INSTALL/bin/centrm centrm
end

=irffactor
 in=88 out=92 fnuc=92238 medit=3 essm=yes nterp=1
 absopt=1 mopt=3  removal=yes  iter=no
 cellfil="het_input"
 ehres=20.0E+03
 subgrxs= 1.0 5.0 10.0 50.0 100.0 500.0 1000.0 5000.0 10000.0 20000.0  end
end

=shell
mv  ft92f001 $RTNDIR/U238_ffactors_lev_m
mv  subgrpdata $RTNDIR/subgrpdata_U238_lev_m
end
```

# APPENDIX B2. SAMPLE GEOMETRY AND COMPOSITION INPUT FOR IRFFACTOR-HET

```
=csas1x  parm=centrm
hetrocells to compute f-factors of U238;
 ft88f001
read composition

'
' ***CELL-1 Composition
'
u-235 1  0  9.39468E-04  293  end
u-238 1  0  2.22624E-02  293  end
o-16  1  0  4.64223E-02  293  end
al-27 2  0  6.02620E-02  293  end
h-1   3  0  1.17012E-04  293  end
o-16  3  0  5.85142E-05  293  end

'
' ***CELL-2 Composition
'
u-235 4  0  9.39468E-04  293  end
u-238 4  0  2.22624E-02  293  end
o-16  4  0  4.64223E-02  293  end
al-27 5  0  6.02620E-02  293  end
h-1   6  0  9.36093E-03  293  end
o-16  6  0  4.68114E-03  293  end

'
' ***CELL-3 Composition
'
u-235 7  0  9.39468E-04  293  end
u-238 7  0  2.22624E-02  293  end
o-16  7  0  4.64223E-02  293  end
al-27 8  0  6.02620E-02  293  end
h-1   9  0  2.34023E-02  293  end
o-16  9  0  1.17028E-02  293  end

'
' ***CELL-4 Composition
'
u-235 10  0  9.39468E-04   293  end
u-238 10  0  2.22624E-02   293  end
o-16  10  0  4.64223E-02   293  end
al-27 11  0  6.02620E-02   293  end
h-1   12  0  3.51035E-02   293  end
o-16  12  0  1.75543E-02   293  end

'
' ***CELL-5 Composition
'
u-235 13  0  9.39468E-04   293  end
u-238 13  0  2.22624E-02   293  end
o-16  13  0  4.64223E-02   293  end
al-27 14  0  6.02620E-02   293  end
h-1   15  0  4.68046E-02   293  end
o-16  15  0  2.34057E-02   293  end

'
' ***CELL-6 Composition
'
u-235 16  0  9.39468E-04   293  end
u-238 16  0  2.22624E-02   293  end
o-16  16  0  4.64223E-02   293  end
al-27 17  0  6.02620E-02   293  end
h-1   18  0  4.68046E-02   293  end
o-16  18  0  2.34057E-02   293  end

'
' ***CELL-7 Composition
'
u-235 19  0  9.39468E-04   293  end
u-238 19  0  2.22624E-02   293  end
```

```
o-16  19  0  4.64223E-02   293  end
al-27 20  0  6.02620E-02   293  end
h-1   21  0  4.68046E-02   293  end
o-16  21  0  2.34057E-02   293  end

'
' ***CELL-8 Composition
'
u-235 22  0  9.39468E-04   293  end
u-238 22  0  2.22624E-02   293  end
o-16  22  0  4.64223E-02   293  end
al-27 23  0  6.02620E-02   293  end
h-1   24  0  4.68046E-02   293  end
o-16  24  0  2.34057E-02   293  end

'
' ***CELL-9 Composition
'
u-235 25  0  4.69734E-04   293  end
u-238 25  0  1.11312E-02   293  end
o-16  25  0  2.32111E-02   293  end
al-27 26  0  6.02620E-02   293  end
h-1   27  0  4.68046E-02   293  end
o-16  27  0  2.34057E-02   293  end

'
' ***CELL-10 Composition
'
u-235 28  0  2.34867E-04   293  end
u-238 28  0  5.56561E-03   293  end
o-16  28  0  1.16056E-02   293  end
al-27 29  0  6.02620E-02   293  end
h-1   30  0  4.68046E-02   293  end
o-16  30  0  2.34057E-02   293  end

'
' ***CELL-11 Composition
'
u-235 31  0  1.17434E-04   293  end
u-238 31  0  2.78280E-03   293  end
o-16  31  0  5.80278E-03   293  end
al-27 32  0  6.02620E-02   293  end
h-1   33  0  4.68046E-02   293  end
o-16  33  0  2.34057E-02   293  end

'
' ***CELL-12 Composition
'
u-235 34  0  5.87168E-05   293  end
u-238 34  0  1.39140E-03   293  end
o-16  34  0  2.90139E-03   293  end
al-27 35  0  6.02620E-02   293  end
h-1   36  0  4.68046E-02   293  end
o-16  36  0  2.34057E-02   293  end

'
' ***CELL-13 Composition
'
u-235 37  0  2.93584E-05   293  end
u-238 37  0  6.95701E-04   293  end
o-16  37  0  1.45070E-03   293  end
al-27 38  0  6.02620E-02   293  end
h-1   39  0  4.68046E-02   293  end
o-16  39  0  2.34057E-02   293  end

'
' ***CELL-14 Composition
'
u-235 40  0  9.39468E-06   293  end
u-238 40  0  2.22624E-05   293  end
o-16  40  0  4.64223E-04   293  end
al-27 41  0  6.02620E-02   293  end
h-1   42  0  4.68046E-02   293  end
o-16  42  0  2.34057E-02   293  end
```

```
'
' ***CELL-15 Composition
'
u-235 43  0  9.39468E-06   293  end
u-238 43  0  2.22624E-08   293  end
o-16  43  0  4.64223E-04   293  end
al-27 44  0  6.02620E-02   293  end
h-1   45  0  4.68046E-02   293  end
o-16  45  0  2.34057E-02   293  end

'
' ***CELL-16 Composition (infinitely dilute; Homo mixture)
'
u-235 70  0  9.3947E-05 293  end
u-238 70  0  1.0E-12    293  end
o-16  70  0  0.046422   293  end
al-27 70  0  0.060262   293  end
h-1   70  0  4.4183E-02 293  end
o-16  70  0  2.2095E-02 293  end
'-------------------------------------------------------

end composition

read celldata

'
' ***CELL-1 Geometry
 latticecell  squarepitch  pitch=1.2620 3 fuelr=0.4025 1
              cladr=0.4759 2   end
 centrmdata  demin=.0001  demax=9.E3 iup=15 npxs=6 end centrmdata

'
' ***CELL-2 Geometry
 latticecell  squarepitch  pitch=1.2620 6  fuelr=0.4025 4
              cladr=0.4759 5   end
 centrmdata  demin=.0001  demax=9.E3 iup=15 npxs=6 end centrmdata

'
' ***CELL-3 Geometry
 latticecell  squarepitch  pitch=1.2620 9  fuelr=0.4025 7
              cladr=0.4759 8   end
 centrmdata  demin=.0001  demax=9.E3 iup=15 npxs=6 end centrmdata

'
' ***CELL-4 Geometry
 latticecell  squarepitch  pitch=1.2620 12  fuelr=0.4025 10
              cladr=0.4759 11   end
 centrmdata  demin=.0001  demax=9.E3 iup=15 npxs=6 end centrmdata

'
' ***CELL-5 Geometry
 latticecell  squarepitch  pitch=1.2620 15  fuelr=0.4025 13
              cladr=0.4759 14   end
 centrmdata  demin=.0001  demax=9.E3 iup=15 npxs=6 end centrmdata

'
' ***CELL-6 Geometry
 latticecell  squarepitch  pitch=1.5728 18  fuelr=0.4025 16
              cladr=0.4759 17   end
 centrmdata  demin=.0001  demax=9.E3 iup=15 npxs=6 end centrmdata

'
' ***CELL-7 Geometry
 latticecell  squarepitch  pitch=2.0581 21  fuelr=0.4025 19
              cladr=0.4759 20   end
 centrmdata  demin=.0001  demax=9.E3 iup=15 npxs=6 end centrmdata

'
' ***CELL-8 Geometry
 latticecell  squarepitch  pitch=2.2621 24 fuelr=0.4025 22
              cladr=0.4759 23   end
 centrmdata  demin=.0001  demax=9.E3 iup=15 npxs=6 end centrmdata

'
' ***CELL-9 Geometry
```

```
 latticecell  squarepitch  pitch=2.2621 27  fuelr=0.4025 25
             cladr=0.4759 26   end
 centrmdata  demin=.0001  demax=9.E3 iup=15 npxs=6 end centrmdata

'
' ***CELL-10 Geometry
 latticecell  squarepitch  pitch=2.2621 30  fuelr=0.4025 28
             cladr=0.4759 29   end
 centrmdata  demin=.0001  demax=9.E3 iup=15 npxs=6 end centrmdata

'
' ***CELL-11 Geometry
 latticecell  squarepitch  pitch=2.2621 33  fuelr=0.4025 31
             cladr=0.4759 32   end
 centrmdata  demin=.0001  demax=9.E3 iup=15 npxs=6 end centrmdata

'
' ***CELL-12 Geometry
 latticecell  squarepitch  pitch=2.2621 36  fuelr=0.4025 34
             cladr=0.4759 35   end
 centrmdata  demin=.0001  demax=9.E3 iup=15 npxs=6 end centrmdata

'
' ***CELL-13 Geometry
 latticecell  squarepitch  pitch=2.2621 39  fuelr=0.4025 37
             cladr=0.4759 38   end
 centrmdata  demin=.0001  demax=9.E3 iup=15 npxs=6 end centrmdata

'
' ***CELL-14 Geometry
 latticecell  squarepitch  pitch=2.2621 42 fuelr=0.4025 40
             cladr=0.4759 41   end
 centrmdata  demin=.0001  demax=9.E3 iup=15 npxs=6 end centrmdata

'
' ***CELL-15 Geometry
 latticecell  squarepitch  pitch=2.2621 45  fuelr=0.4025 43
             cladr=0.4759 44   end
 centrmdata  demin=.0001  demax=9.E3 iup=15 npxs=6 end centrmdata

'
' ***CELL-16 Geometry (infinitely dilute; Homo mixture)
infhommedium  70   end
 centrmdata  demin=.0001  demax=9.E3 iup=15 end centrmdata

'-------------------------------------------------------
end celldata

end
```

# APPENDIX C1. SAMPLE INPUT OF MPACT

```
CASEID pwr_06k_m

MATERIAL
  mat  1 2 10.36 g/cc 600 K    \ 92235 9.39468E-04
                                 92238 2.22624E-02
                                  8001 4.64223E-02
  mat  2 4 6.56 g/cc 600 K     \ 13027 6.02620E-02
  mat  3 0 0.661 g/cc 600 K    \  8016 2.34057E-02
                                  1001 4.68046E-02

GEOM

 !Loads pin modular ray tracing and all pin types
 !Module 1 - common pin geometry

 file base_bench1_geom.inp

 !Define lattices, assemblies and core
 lattice 1 2*1
  1

 assembly 1
  1

 core 360
  1

XSEC
  addpath .
  xslib ORNL mpact51g_70m_v4.1m0_test.fmt

OPTION
  bound_cond 1 1 1 1 1 1
  solver 1 2
  ray 0.02 CHEBYSHEV-YAMAMOTO 8 3
  !parallel 1 1 1 16
  conv_crit 2*1.e-6
  iter_lim 2000 2 3
  scatt_meth  P2
  vis_edits F
  validation T C



  !Ray tracing module dimensions
   mod_dim 1.262 1.262 1.0

   !Pin mesh
    pinmesh 1 cyl  0.4025 0.4759 0.575 / 1.262 /  1.0  /  1 1 1  / 8 8 2*8 /  1  !Pin mesh

  !  Material 1:  Fuel
  !  Material 2:  Clad
  !  Material 3:  Water

   pin 1 1 / 1 2 3 3! same for every problem, just different materials

  !Pin modular ray tracing
   module 1 3*1
    1
```